

Scales Formation Inhibition on Top of C-Steel in Sour Media; A Chemical and Electrochemical Study

Noora Al-Qahtani^{1,2*}, Jiahui Qi¹, Aboubakr M. Abdullah², Nicholas J. Laycock³ and Mary P. Ryan¹

¹Department of Materials, Imperial College London, Exhibition Road, London, UK

²Center for Advanced Materials, Qatar University, Doha-Qatar

³Qatar Shell Research and Technology Centre, Doha-Qatar

Abstract

Corrosion control in sour environments is a serious challenge for oil and gas industry in sour media. One of the approaches to mitigate such problem is to use corrosion inhibitors (CI). The selection of a single or a mixture of CIs for a particular oil or gas production, transportation or storage facility depends on different parameters e.g. the ratio between carbon dioxide and hydrogen sulfide, pH, pressure, temperature, and brine chemistry where different kinds of iron sulfide and/or iron carbonate layers can be formed. To select the right corrosion inhibitor/s, it is highly crucial to understand the mechanism of corrosion of C-steel and its inhibition in H₂S systems in absence and presence of CIs [1,2].

In this work, the electrochemical behavior of C-steel in (i) deionized water (DIW) and (ii) different NaCl solutions were examined in an H₂S system. A series of experiments were conducted at different temperatures and two concentrations of inhibitors (A and B). The corrosion behavior of C-steel was investigated by measuring the open circuit potential (OCP), linear polarization resistance (LPR), and potentiodynamic polarization (PDP) in addition to scanning electron microscopy (SEM) coupled with an energy dispersive X ray (EDX) besides Raman spectroscopy (RS). The results have shown that the corrosion rate of C-steel gradually decreased then stabilized with time in the inhibited solutions. The inhibition efficiency was found to increase in the presence of both types of inhibitors with temperatures. Surface analysis shows that no film of corrosion products existed. In fact, CIs controlled the corrosion process and prevented passive film formation (iron sulfide), even in the presence of H₂S in all tests.

Keywords: Scale formation • Mechanism • Sour environment • Environmental factors

Introduction

Iron and its alloys are generally utilized in several tenders; most of it is as pipeline material because it has suitable properties which can be broadly utilized in natural gas, and crude oil pipelines in the oil and gas manufacturing. Nevertheless, it is vulnerable to critical degradation by H₂S contained in the transported fluid that always exists in both natural gas and crude oil [3]. In fuel manufacture, a sour brine is mainly used (NACE ID 182) and usually utilized to execute corrosion research and the assessment of Corrosion Inhibitors (CIs) [4]. Significant attention has been given to the usage of inhibitors due to it being one of the best approaches controlling corrosion, specifically in acidic media. It prevents the iron dissolution 'reducing metals loss in areas and acid consumption and therefore reduces the corrosion rate to a noticeable extent. Corrosion inhibitors for metal are chemicals once added in slight quantities to corrosive media, suppress the metal dissolution rate [5].

Investigation of CIs has been primarily concentrated on the inhibitor framework link with its mechanism and adsorption features. It has been detected that adsorption is hugely influenced by particular physicochemical properties of the CI molecules, such as groups of atoms (i.e. functional sets), aromaticity, steric impact, electron density of atoms (donor), and the

π -orbital type of donating electrons. Besides, it is contingent on the electronic framework of the molecules and the ability to interface between the inhibitor and the iron. Hence, the effectiveness of any compound is primarily reliant on its strength to be adsorbed on the iron surface enriching the surface with electrons [6]. CI can be a single (organic) or a compound/solvents mixture of compound surfactant or compound co solvents [7].

CI can be classified into three groups: (I) Inorganic Substances such as Rare Earth Metal (REM) salts, borates, silicates, and molybdates. (II) Organic Compounds such as thioglycollates, phosphonates, sulfonates, carboxylic acids/salts (amino acids, fatty acids, gluconates), vitamins, pigments, antibiotic/antifungal drugs (e.g., imidazole compounds), alkaloids (nicotine, caffeine). (III) True 'Green' Inhibitors, for example, several herbal extracts (water, alcohol or acid extracts) [7]. Over the last decade, commercial inhibitors have been manufactured and working effectively to impede corrosion of iron in sour system. Those products contain at least one of the subsequent surfactants: fatty (acids, amines, diamines, amido amines or imidazolines), (quaternary oxyalkylated) amines, other amine derivatives, and oxygen, sulfur or phosphorus containing compounds which act as film forming inhibitors [8]. The most efficient inhibitors used in the industry contain heteroatoms. For example, nitrogen, sulfur, and/or oxygen and also the hydrophobic hydrocarbon series in the structures create a decrease

***Address for Correspondence:** Noora Al Qahtani, Center for Advanced Materials, Qatar University, Doha-Qatar, Email: noora.alqahtani@qu.edu.qa

Copyright: © 2021 Noora Al Qahtani, et al. This is an open-access article distributed under the terms of the Creative Commons Attribution License, which permits unrestricted use, distribution, and reproduction in any medium, provided the original author and source are credited.

Received date: 30 April, 2021; **Accepted date:** 14 May, 2021; **Published date:** 21 May, 2021

in corrosion rate of metals, although this has not been fully investigated yet over the past few decades. While many synthetic composites revealed good anticorrosive achievements, many of them were extremely toxic to both humans and the environment. Therefore, strict ecological laws and increasing environmental consciousness have led experts to concentrate on the improvement of 'green' alternatives to moderate corrosion [5,9–11].

Many types of research have been carried out on the impact of CIs on the C-steel corrosion in several situations. Recently, several investigations have been carried out on the CI of metals. Huilong et al. [9] examined corrosion inhibitor of steel in HCl acid media using bis quaternary ammonium salt as a corrosion inhibitor. The investigation was in 1M HCl with the adding many CI concentrations at several immersion times from 2 to 10 hours and at a constant temperature of $25 \pm 0.5^\circ\text{C}$ further characterised by a weight loss scheme, electrochemical systems (current potential curves) and surface analyses. The outcomes were compared to a commercial corrosion inhibitor used in industry for sour media. The consequences displayed good prevention action by the inhibitor. Also, the impact of Fe^{3+} ions on IE% in sour system was studied signifying that ferric ions can catalyse the corrosion of metal. The IE rise with the CI amounts is, nevertheless, temperature-independent because of the development of a stable deposit firmly connected to the iron surface.

Moreover, Shahabi et al. [12] studied the theoretical and electrochemical investigation of the inhibition outcome of two synthesised CIs on CS in sour solutions. They did many measurements using mass loss, Tafel polarisation technique, electrochemical impedance spectroscopic and fast fourier transform continuous cyclic voltammetry. The results demonstrate that the studied organic compounds of CI drop the corrosion rate and the inhibition effectiveness grows with rising the concentration inhibitors. The inhibitors were found to be of the mixed category or adsorptive inhibitors with a mainly anodic effect.

Also, the experimental and theoretical investigation was studied by Hemapriya et al. [13] using two synthesised inhibitors that were derived from benzothiazines for corrosion inhibition of CS in an acidic medium ($1\text{M H}_2\text{SO}_4$). They used weight loss measurements for corrosion inhibition efficiency (IE%), polarisation technique (potentiodynamic), impedance spectroscopy, SEM and FT-IR spectroscopy. The data obtained showed that the IE% improved with inhibitor concentration and dropped at higher temperatures. The inhibitors were found to be influencing both cathodic hydrogen progression and anodic metal dissolution.

The temperature effect on the inhibition in acidic media for CS was examined by Yahya et al. [14] using one type of inhibitor; lignin. He performed weight loss corrosion assessments at a different range of temperatures (30°C - 70°C). The finding was that the efficiency (IE%) of lignin was reduced while the temperature was raising from 60°C - 70°C . Subsequently, in the range from 30°C - 50°C (lower temperatures) the IE% was high that casue by the adsorption of lignin on the surface.

Conversely, the very minimal effect on quaternary ammonium mixtures as inhibitors for metal corrosion in sour system has been addressed. Although slight progress has been accomplished in sympathetic H_2S corrosion mechanisms, the kinetics of the inhibition progression required to measure formulations for essential protection remains incomplete. Therefore, a systematic approach to the inhibition and adsorption behaviour of imidazole based inhibitors is essential. In addition to our work on the improvement of CIs in acidic system, we have examined the preventing impact on the C-steel corrosion in HCl media using three altered investigational performances (for instance open circuit (OPC) linear polarization resistance (LPR) and polarization measurements) and surface analytical techniques for characterization of the corrosion inhibitor film. These techniques assess corrosion routes and inhibitor enactment in many concentrations and at several temperatures.

Corrosion inhibitor overview and qualification

Qualification and selection of corrosion inhibitor for oil and gas field applications include the requirement of corrosion inhibitors in the laboratory is explained in ASTM standards [15]. Based on our communication with an industry expert from Shell, several different inhibitor formulations are offered in the market, and the choice for a particular application is classically based on a programme of selection and qualification testing in the laboratory. Such programmes are proposed to guarantee that the selected inhibitor will offer acceptable protection to the process in all probable environmental situations that are possible to be developed throughout the project lifetime. Since it is not typically applied to trial all possible combinations, a selection is regularly made based on the presumed 'worst case' conditions [16]. Some features might influence the performance of inhibition in pipelines. Factors, for instance, are the nature of inhibitor, operating conditions of a system as temperature and pressure, oil/water partitioning, water chemistry and flow situations and the technique by which it is added have been generally studied. In the past, less awareness was given to some aspects, for example, the microstructure and element of the CS, the kind of corrosion results shaped on the CS surfaces, inhibitor adsorption on postponed components in the generated water and inhibitor increase on boils and water/oil drops [17]. The usual main acceptance criterion for such an inhibitor is evaluated the corrosion rate (general and pitting) and stability. The essential principles are that the general corrosion percentage must be under 0.1 mm/y under numerous operating conditions. Likewise, for pitted corrosion, to get a 'pass', it needs to be less than 0.18 mm/y , which corresponds to a $10\ \mu\text{m}$ pit formed in 500 hours of required testing. Minor properties are, for instance, emulsification and foaming tendency and long term storage stability, condensate stabiliser stability and compatibility with other chemicals [16]. All corrosion inhibitors used are scale inhibitors that manufactured by Baker Hughes and are typically injected into oil and gas pipelines. CIs named as A and B correspond to applicants, and two commercial inhibition supplied by Qatar Shell via various vendors for qualification for a specific field as is seen in Table 1 [16,18,19].

Inhibitor	A	B
Trade Name	CRONOX™CRW9258/SSWL0228	CGW80742P
Company	Baker Hughes	
Information	It is a water-soluble/oil insoluble organic corrosion inhibitor. It is effective against corrosion caused by hydrogen sulfide, carbon dioxide, organic and mineral acids, salts, etc. This product exhibits excellent solubility in a variety of high dissolved solids content brines.	It is a water-soluble organic corrosion inhibitor. It is effective against corrosion caused by hydrogen sulfide, carbon dioxide, organic and mineral acids, and salts commonly found to cause extensive corrosion in oil-field production.
Features and benefits	A general-purpose corrosion inhibitor where high temperature and water solubility are desired.	A general-purpose corrosion inhibitor where pitting in sour systems is a potential problem.
Rate	Typical continuous injection rates are 100 to 500 ppm based on total water being treated and the severity of corrosion experienced	Typical continuous injection rates are 200 to 1000 ppm based on the total water being treated and the severity of corrosion experienced.

Specific gravity at 60 °F (16°C)	1.02	Approx. 1.0
Typical density at 60 °F (16°C)	8.51 lbm/US gal (1019.72 kg/m ³)	-
Flash point	SFCC 87.8 °F (31°C)	Approx. 16°C [PMCC]
Pour point	-20 °F (-29°C)	-

Table 1. Summary of the CI used in qualification work [20,21]

Materials and Methods

The influence of inhibitors on the corrosion was performed using CS coupons with a combination (wt.%) of 0.02% S, 0.05% P, 0.12% Mn, 0.17% Si, 0.20% C and equilibrium Fe were slashed into 1.00 cm³ features for the electrochemical investigates. Prior to measurements being taken, the specimens were degreased with ethanol and cleaned with demineralised water. The area of bare surface of the electrochemical sample was 1 cm²; however, the rest was implanted in an epoxy resin. Later the coupons, the working electrodes, were submerged in an electrochemical cell including 20 ml of studied solution. All investigations were completed at ambient temperatures (RT), 50, and 80°C, and atmospheric pressure. Operations were performed on 4 different media: DIW with and without salts such as NaCl (0.01 M, 0.1 M, and 1 M). Two kinds of corrosion inhibitors (A and B) were used with different concentrations and added to the media. Table 2 displays the test circumstances and demonstrates the experimental procedures. The electrochemical cell was made up of a three electrode structure and consisted of CS (WE), a Pt counter electrode (CE) and an MSE reference electrode (RE). As the iron specimen was obscured in the electrolyte, the OCP was measured until the specimen accomplished a steady potential E_{corr} (usually after one hour). Afterwards, linear polarisation measurements were started (± 20 mV, polarization scan rate 0.15 mV·s⁻¹) with the aim of determining the corrosion rate (CR) and the assessment of polarization resistance (Rp). Lastly, the routine of the polarization curve was executed recording the curves in the series - 250 mV_{vs} OCP to 100 mV_{vs} RE with a polarization rate of 0.5 mV·s⁻¹. In the situation of polarization technique, the relative establishes the inhibition efficiency (IE%) [22]:

$$IE\% = \frac{I_{corr} - I_{corr}(inh)}{I_{corr}} \times 100$$

Where I_{corr} and $I_{corr}(inh)$ are the corrosion current density amounts without and within the inhibitor, individually specified by extrapolation of cathodic and anodic Tafel lines to the corrosion potential [22], this examination technique was aimed to inspect the influence of inhibitors on the H₂S

corrosion of CS. After the test, the samples were utilised for further *ex situ* studies. The morphology and compositions of corrosion specimens from each period were explored with Raman spectroscopy (RS), scanning electron microscopy (SEM), and energy dispersive X ray spectroscopy (EDS).

Material	Carbon steel
Solution	Deionized water, 0.01 M NaCl, 0.1 M NaCl, and 1 M NaCl
Inhibitor type and concentration	A and B @50 ppm and 500 ppm
Temperature	Ambient temperature, 50°C, and 80°C
Pressure	Atmospheric

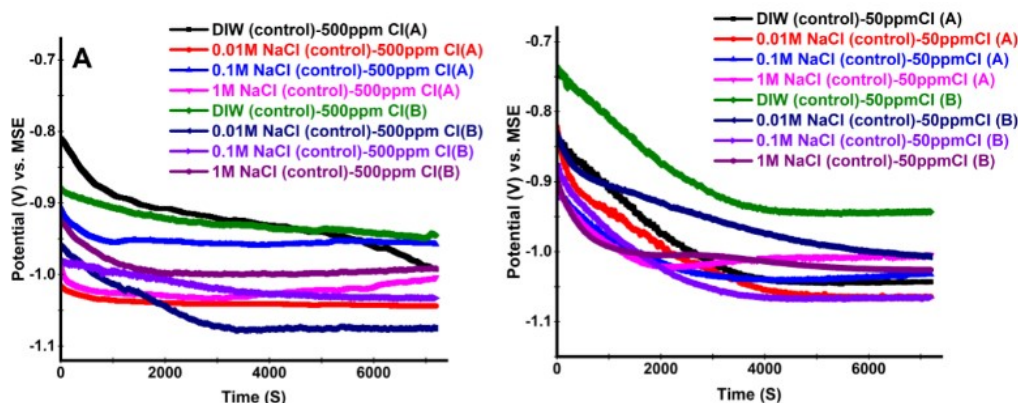
Table 2. Test conditions

Results and Discussion

In the present work, electrochemical properties were determined from different tests in two stages of adding the corrosion inhibitors (CIs) concentration. In stage 1, a solution of the electrolyte was mixed with CIs, and the stage 2 was adding the CI after 2 h of the test where the samples were immersed in a solution of electrolyte saturation mixed with H₂S.

Open Circuit Potential (OCP) measurements with time

OCP was measured to be 'stability; rest; or E_{corr} - corrosion potential,' which has no current passed. The potential value of the iron electrodes obscured in a media was distinguished against the MSE electrode as a function of contact time in both the absence and existence of altered amounts from CIs. The achieved potential–period plots are demonstrated in Figure 1- Figure 4. A noticeable fall in E_{OCP} is detected with the adding of CI in either DIW solution or chloride solutions. It characterizes the variation of E_{OCP} of C-steel that was examined carefully at various concentrations of inhibitors, both with and without the presence of H₂S.



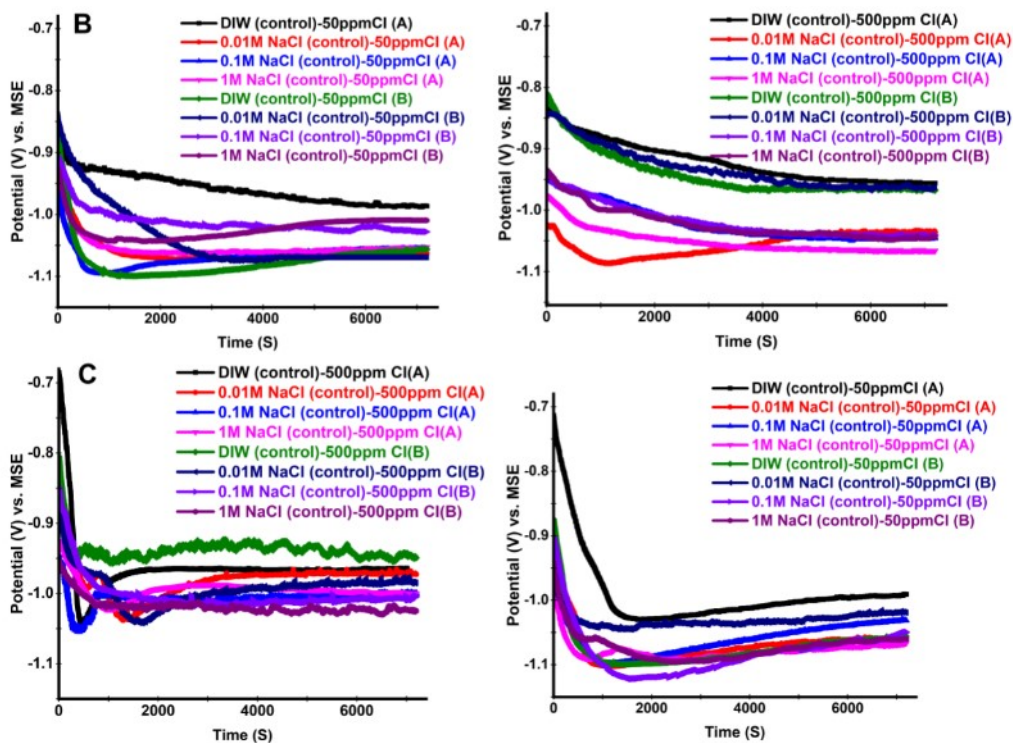


Figure 1. Change of the E_{ocp} as a function of period noted for a CS electrode control solutions without H_2S in the system @A: RT, B: 50, and C: 80°C

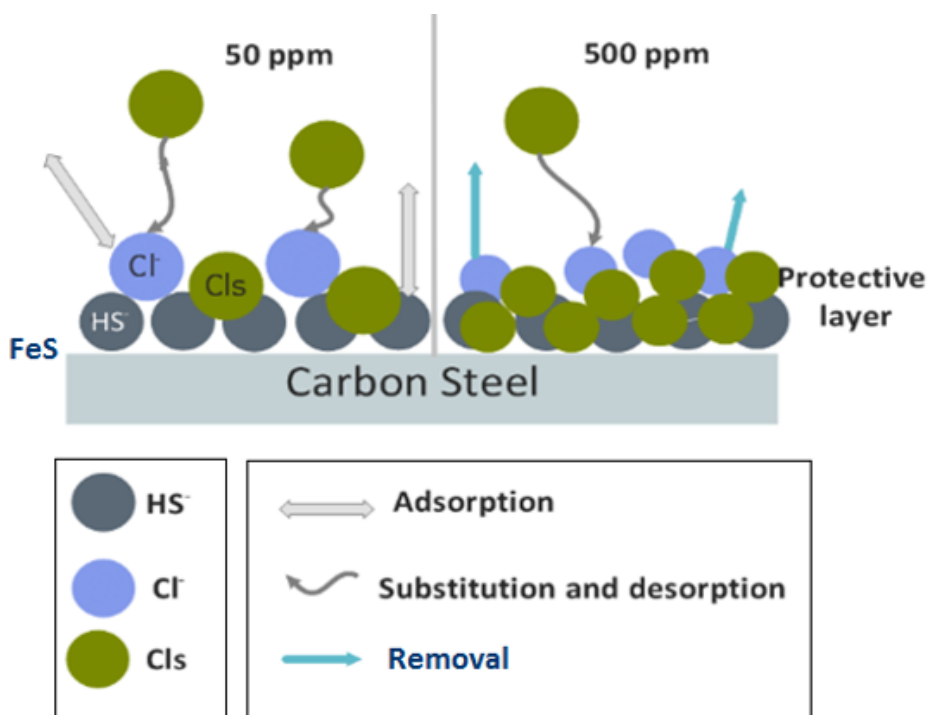


Figure 2. Schematic diagram of CS with adding Cls in the H_2S system @ the beginning of the reaction.

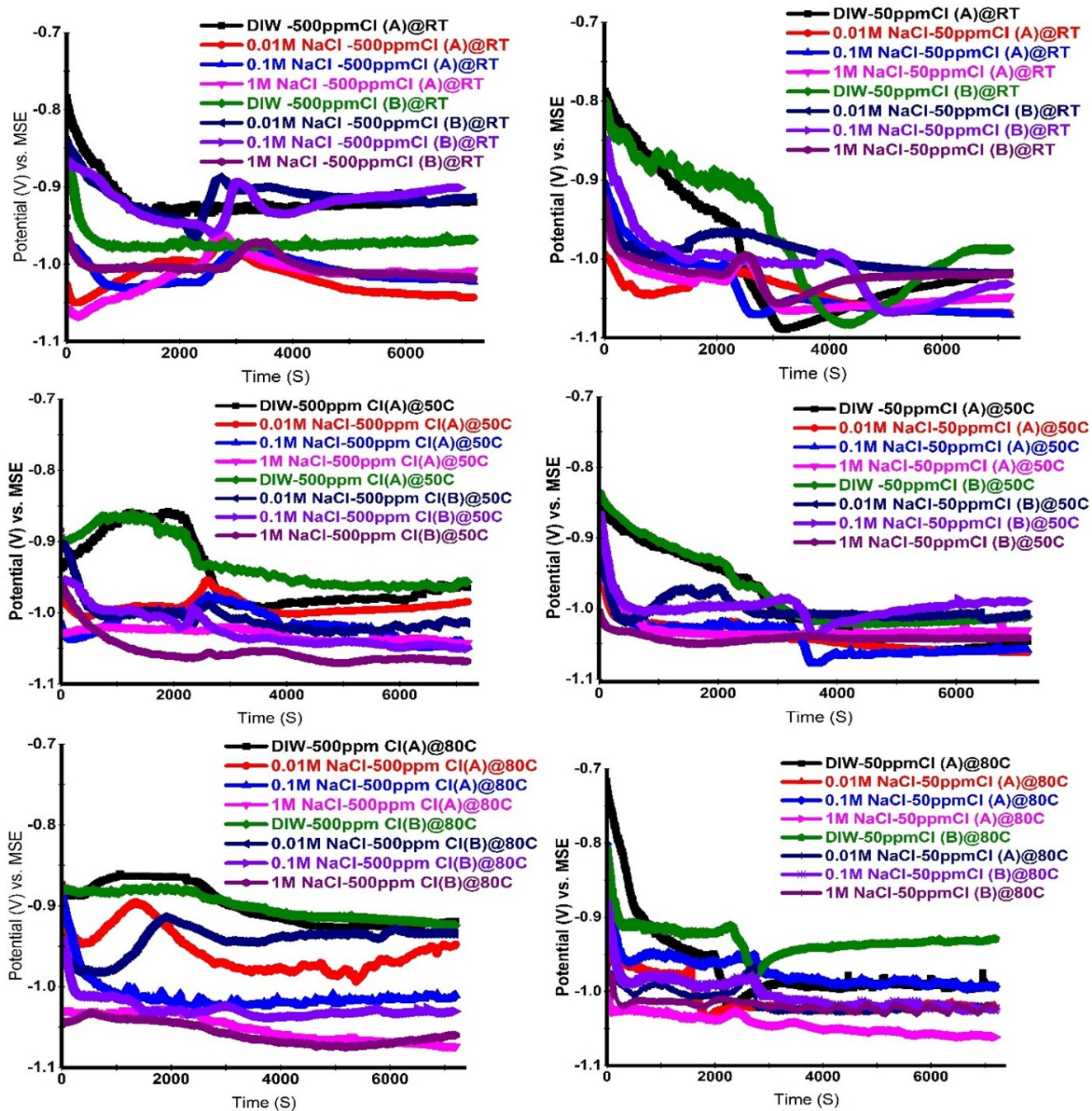


Figure 3. The free corrosion potential variation of CS by adding 50 and 500 ppm of Cls in different solution + H₂S in the system @ different temperatures

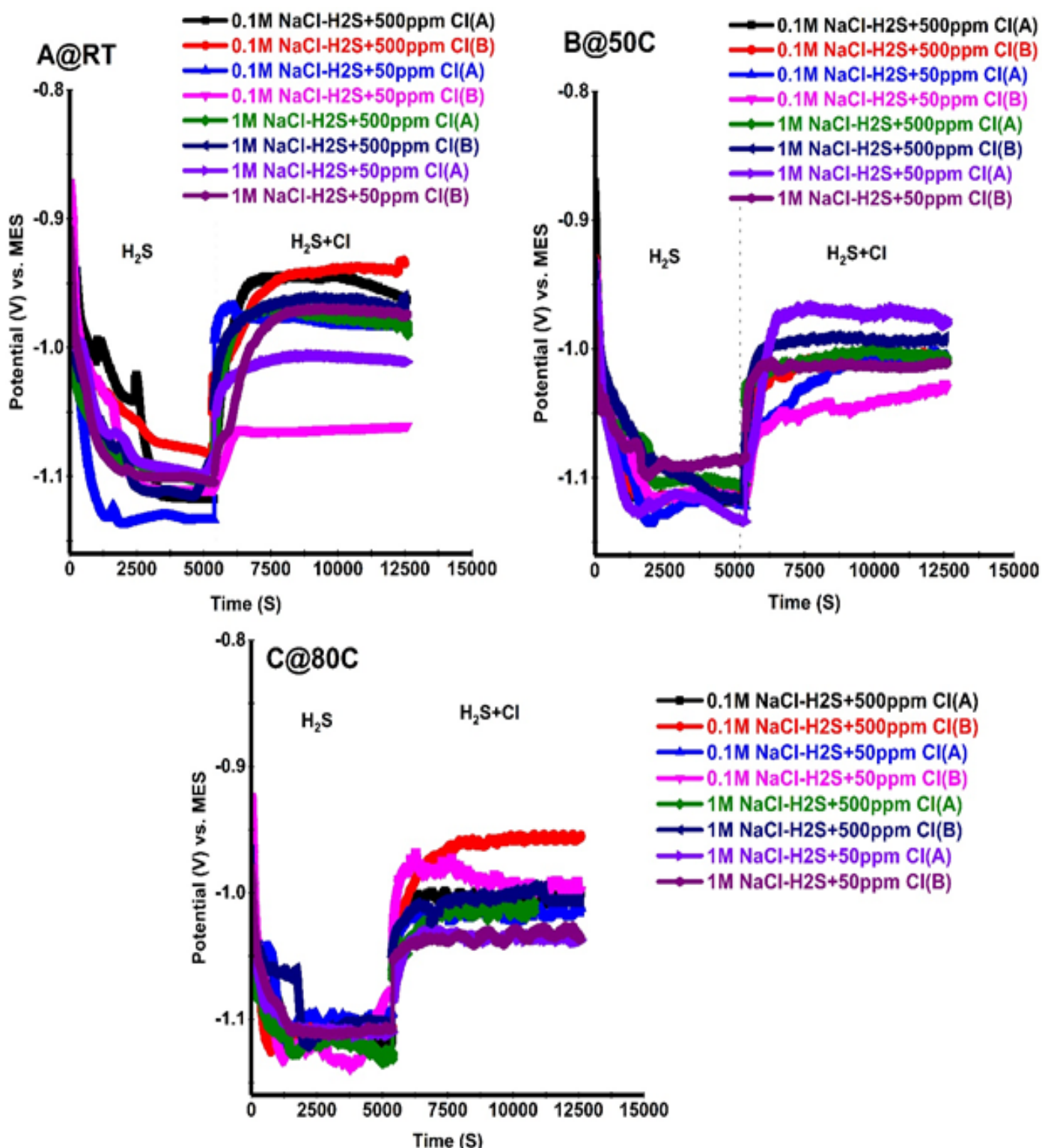


Figure 4. The change in open circuit potential as a function of different concentrations and temperatures for C- steel in NaCl solution before and after adding Cl⁻

Stage 1: Adding the Cl at the beginning of test reaction: The E_{OCP} of CS was followed over a 2 h period of time using the electrode immersion technique in the test media at several temperatures and varying concentrations of Cls. In the absence of H_2S in the system, i.e., control test (Figure 1), the steady state amount of E_{OCP} initially decreased with time and finally extended to stable values in 500 ppm. Even by increasing the temperature, the potential dropped gradually to a further negative value starting from the beginning of the observation period until a steady state reading was accomplished. When the E_{OCP} values were reached the steady state, the inhibitors have formed a film. This steady state potential, which was accomplished very quickly (subsequent around 600 s of immersion), and inhibition film that was existing on the bare alloy surface (seen in SEM result).

In all the cases of 50 ppm, the E_{OCP} trend is comparable, which means the E_{OCP} value in the beginning dramatically decreased to further noble values, and then achieves a plateau stage. In the primary estimate, this shows that the response reduces with moment and later gets a steady state level contained by the time interval stated and representing the adsorption of Cl on the CS surface. The stabilise value of E_{OCP} in the control solution of Cl, which displayed that all trends had that same range of E_{OCP} .

Meanwhile, the E_{OCP} followed from Cls in the presence of H_2S in the system (Figure 3), have a very different trend in DIW and NaCl from what was observed in the controlled system. The E_{OCP} values in RT with @500 ppm Cls for DIW solutions had high initial values that salt solutions and decreased continuously with time. The potential value moved straight to the negative path and ultimately achieved a constant rate. As for the NaCl solution @RT-500 ppm Cls, it decreased immediately, followed by a gradual increase to create a peak value and then reduced slightly more before staying at a low E but constant rate over the remainder of the assessment. Furthermore, the E_{OCP} reading in DIW at a higher temperature had a high top value, and a slow decline until reached the steady state potential. The value of steady state became more negative at high temperatures. This showed that the combinations protected the iron corrosion in DIW. However, in NaCl solutions, it demonstrated the insignificant influence of temperature on free potentials. In the E_{OCP} regime, however, the trend decreased at a higher temperature, and the transition peaks lessened over time and then decreased suddenly before reaching stable values. Even at the end of an experimental period of 7000 s, the rate of decline in E_{OCP} is quite considerable. The difference in the shape of the corrosion action is because the protective layer of the alloy or metal is formed. This is remarked when the potential becomes noble and then starts to decrease with Cls at room temperature. With raising the temperature, the potential connection to the general corrosion process has fallen because E_{OCP} is more negative, representing the protective appearances of the films. Additionally, the shift of initial E_{OCP} values in a positive trend with a high aggregate intensity of inhibitors, recommends the strength of the surface coating for inhibitors, as shown in Figure 2 [23,24].

It is observable from Figure 3 at 50 ppm; that the addition of H_2S in either DIW or NaCl solution moves the E_{corr} to more negative values (steady state potential) while altering the overall structures of the E/t curve, i.e., having some transition peaks. By raising the temperature, an effect on E_{OCP} and becomes more active, and the transition peak starts to disappear and speeds up the reaction. However, upon raising the concentration of salt to 1 M, a new curve characteristic was noted, which was dependent on the concentration at room temperature. Also, the E_{OCP} moved very quickly to a less negative quantity and have a maximum value than other salt solutions. After a specific time 4000 s, the potential tried to reach a steady state. With rising the temperature, the peak still there with fewer appearances than RT. Alternatively, the data from the previous chapter, carbon steel submerged in inhibitor free media, showed that the free potential is more negative than inhibition solution, and E_{OCP} decreased with time and stabilized to low values for all solutions.

These outcomes verified that two counter acting progresses on the

surface. The initial process created the formation of a corrosion layer that was iron sulfide, and it decreased the potential to more negative values (i.e., active path). The next process was through a protective adsorbed Cl film on the surface of the electrode, and therefore, corrosion occurred as was evidenced by the fluctuations in the E_{OCP} to more noble values. The competition between these two opposing behaviour routes might clarify the form of the peak (max. point) in the OCP against time plots. Besides, the former moved in 1 M of NaCl to a smaller value of the peak, which was caused by corrosion inhibition achieving a highest, and, following a particular time, the potential fell to make a sensible, stable value because of metallic dissolution. These results show that 50 ppm of Cls in DIW, 0.01, and 0.1 M NaCl is not sufficient to confirm high level corrosion inhibition, as shown in Figure 4. Moreover, the progressive, positive change of steady state potential with rising amount of NaCl may designate that the ability to prevent the acidic deterioration of CS is increased; also, it might induce pitting [25].

Stage 2: Adding the Cl after H_2S exposure: The results from this stage are demonstrated in Figure 4, the corrosion potential was recorded for 4 h in an H_2S system, and after 1.5 hours, Cls were injected in 0.1 M and 1 M NaCl solutions. The free potential variation in all cases with present H_2S was similar for all the samples. Initially, the potential presented approximately the same value -0.8 to -1.1 mV, and it was observed to decrease in the E_{OCP} during the first 2400 s and then further dropped with increased immersion time before reaching minimum stabilisation in the potential for 5400 s. This means E_{OCP} was remarked to decline as a function of period for all mediums that continued in all cases.

After injecting the Cls into the solutions, the potential jumped dramatically into the direction of the more noble potential for the remainder of the experiment. The E_{OCP} started to fall and showed moderately small variation growths as the time increase, thus leading to the continuous practical potential at the end of the time at almost 15000 s. At high temperature, the behaviour of CS with Cls is quite similar; the E_{OCP} initially increases up to 6000 s. For the next 6000 s the potential remained within -0.95 to -1.1 mV. Later, a stable value of E_{OCP} followed this phase for the rest of the experimental time. We can summarise that from stage 2, all quantities were carried out until the steady state potentials were achieved. It was paramount that the potentials of the electrode immersed in the media had extra negative potential initially, giving rise to a more negative constant value. Adding inhibitor particles to the sour solution after exposure of the sample produced a considerably positive shift in the E_{corr} because of the protective Cl film formation on the iron surface [26].

Potentiodynamic Polarisation Measurements (PDP)

Stage 1: Adding the Cl at the beginning of the reaction: Formerly starting the test, WE were immersed in the H_2S solution for 1800 s. Wait for a steady state of E_{OCP} was required before each PDP run as Figure 5. Focusing on the PDP data acquired in DIW, 0.1 M, and 1 M NaCl, there was a substantial change in the E_{OCP} with Cls concentration. It displayed the evolution of E_{OCP} with time for metal electrodes in the solution with the existence of numerous Cl concentrations and temperatures. An explicit modification in the OCP time behaviour and, specifically, an anodic displacement of E_{OCP} was detected with a positive shift by raising the temperature. The anodic and cathodic polarization behaviour of CS in Cls inhibited solutions were documented after 30 min of exposure at ambient temperature, 50°C, and 80°C. These data of E_{OCP} does not match the steady state from OCP analysis. Plotting E vs. log i curves (Figure 6) has resulted out in the Tafel region for assessment of corrosion kinetic parameters, which are listed in Table 3. The inspection shows that it is strongly evident that adding an inhibitor to the medium affected both the anodic and cathodic measures of the I_{corr} and the E_{corr} was shifted in positive value direction with a more reduction of anodic currents in contrast to cathodic ones. The anodic move in E_{corr} was in agreement with the favoured inhibition of the anodic response. Associating the polarisation behaviour by increasing the temperature of the Cl, resulted in decreasing the I_{corr} . Meaning, both anodic iron dissolution and

cathodic reactions producing hydrogen gas were affected by Cl.

Additionally, the data show that with the adding of both inhibitors in DIW and with the rise in the amount of NaCl, E_{corr} was changed between 60–108 mV with the major cathodic process (is activation controlled) compared to the uninhibited solution which had a range of 98-116 mV. It is reported, that if the displacement in E_{corr} on the addition of inhibitor is greater than 85 mV with respect to E_{corr} of the blank (uninhibited solution), the inhibitor may then be classified as a cathodic or anodic type and if the displacement is less than 85 mV, then the inhibitor may be regarded as mixed type [11,27]. Therefore, the consequences achieved show that a shift in E_{corr} value in the positive trend in 500 ppm inhibitor once the temperature was enhanced indicated that both inhibitor compounds predominately worked as mixed kind inhibitors. In addition, the results recommended that the add on of inhibitors to DIW and salt solutions pointed towards the fact that the inhibition technique is linked to a single response spot preventing

without changing the anodic and cathodic response mechanisms. Likewise, both I_{corr} and CR for DIW and NaCl were experimentally altered by adding the inhibitors, and in consequence, the inspected inhibitors affected both. This was recognised by the observation of a thin layer of FeS, thus proving that the surface of the iron specimens after the electrochemical investigation is not as protected and is shown back to the schematic figure of adsorption Figure 6. It can be assumed that utilized concentration is not appropriate for active corrosion inhibition, as shown in I_{corr} data [28]. The addition of the inhibitor did not affect the hydrogen reduction reaction, and the decrease of H^+ ions at the iron surface revenue sites occurred mostly due to a charge transfer process. The inhibitor molecules were initially adsorbed onto the surface and then reduced the number of the response spots on the metal surface. In this manner, the surface zone subjected to H^+ ions were reduced even though the dissolution reaction behavior was the same. Hence, the addition of the inhibitor did not alter the mechanism of the corrosion on the surface [11].

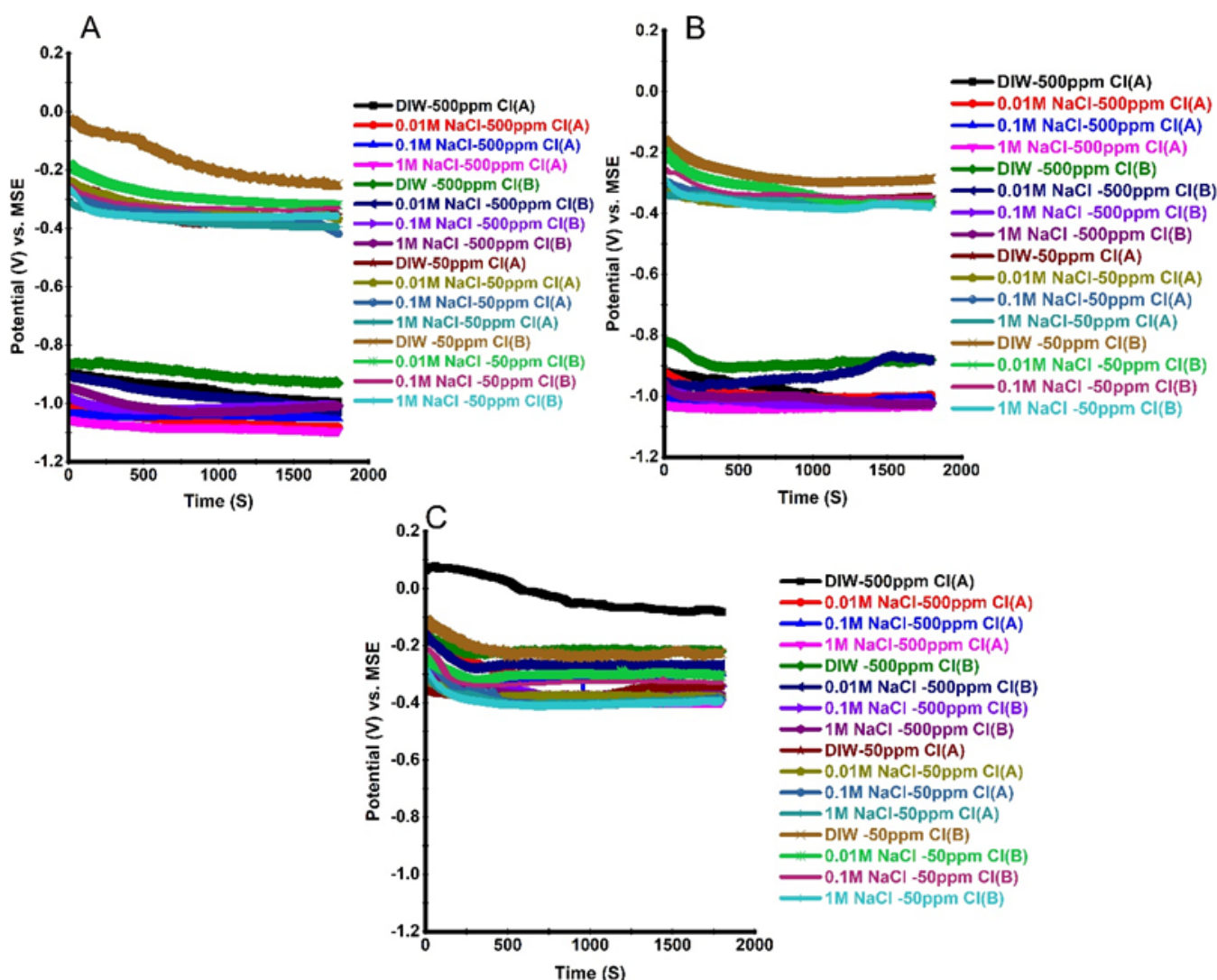


Figure 5. EOCP for the 1800 s of all solutions with adding Cls in the H₂S system @ A: RT, B: 50, and C: 80°C

Test Solutions	E _{corr} (V/MSE)			I _{corr} (μA/cm ²)			CR (mm/y)		
	RT	50°C	80°C	RT	50°C	80°C	RT	50°C	80°C
DIW	-0.98	-1.16	-1.13	21.83	1.98	10.6	0.25	0.02	0.12
DIW-500ppm Cl(A)	-0.91	-0.91	-0.71	1.59	3.82	19.89	0.02	0.04	0.23
DIW-500ppm Cl(B)	-0.95	-0.98	-0.63	0.67	3.24	2.82	0.01	0.04	0.03
DIW-50ppm Cl(A)	-1.01	-0.99	-1.01	4.14	3.98	20.27	0.05	0.05	0.23

DIW-50ppm Cl(B)	-0.92	-0.94	-0.87	14.18	5.04	15.47	0.16	0.06	0.18
0.01M NaCl	-1.12	-1.13	-1.13	2.49	7.75	12	0.03	0.09	0.14
0.01M NaCl-500ppm Cl(A)	-1.06	-0.97	-0.9	3.35	7.07	6.04	0.04	0.08	0.07
0.01M NaCl-500ppm Cl(B)	-1.08	-0.85	-0.93	0.31	2.01	7.62	0.01	0.02	0.09
0.01M NaCl-50ppm Cl(A)	-1.1	-1.02	-1.01	2.18	7.21	14.38	0.03	0.08	0.17
0.01M NaCl-50ppm Cl(B)	-0.97	-0.99	-0.97	2.86	3.87	13.09	0.03	0.04	0.15
0.1M NaCl	-1.11	-1.16	-1.12	9.72	1.49	11.5	0.11	0.02	0.13
0.1M NaCl-500ppm Cl(A)	-1.06	-0.96	-1	9.29	1.9	18.47	0.11	0.02	0.21
0.1M NaCl-500ppm Cl(B)	-0.97	-1.03	-1.01	0.29	0.78	22.87	0	0.01	0.26
0.1M NaCl-50ppm Cl(A)	-1.09	-1.03	-1.34	3.84	1.36	15.39	0.04	0.02	0.18
0.1M NaCl-50ppm Cl(B)	-1.25	-0.97	-0.98	7.02	1.42	18.87	0.08	0.02	0.22
1M NaCl	-1.15	-1.16	-1.15	1.79	4.61	17.5	0.02	0.05	0.2
1M NaCl-500ppm Cl(A)	-1.09	-0.98	-1.07	1.31	3.34	3.39	0.02	0.04	0.04
1M NaCl-500ppm Cl(B)	-0.99	-1.03	-1.07	0.21	1.85	7.65	0.01	0.02	0.09
1M NaCl-50ppm Cl(A)	-0.8	-1.04	-1.06	1.57	9.81	12.29	0.02	0.11	0.14
1M NaCl-50ppm Cl(B)	-0.92	-1.08	-0.99	2.91	3.13	18.92	0.03	0.04	0.22

Table 3. Electrochemical polarisation parameters for carbon steel corrosion at a different temperature in the presence of H₂S from Figure 6

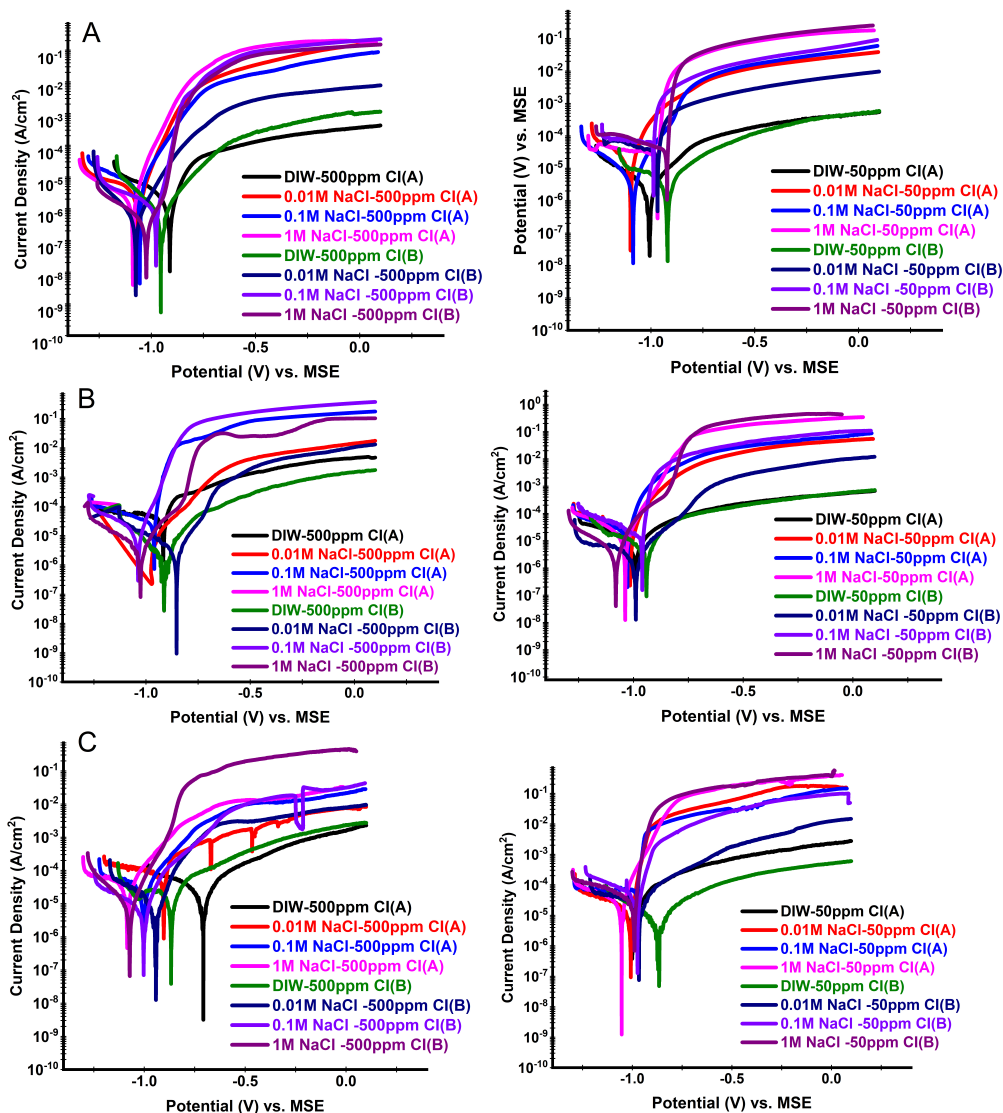


Figure 6. Potentiodynamic polarization curves of different Cl solution @ A: RT, B: 50, and C: 80°C

Linear Polarisation Resistance (LPR)

This test was designed to follow the progress of the E_{corr} and CR as functions of time. All parameters for the conditions were taken from the linear polarisation resistance profiles in Versa Studio and Ivium soft program. The LPR results and analysis are illustrated in Figure 7, which is

consistent with the E_{ocp} findings that explained before in this chapter. The dataset was derived from numerous purging and solution environments to show an overall trend with regards to Cl and temperature. The temperature was crucial to the process of corrosion as changes happen on the inhibited iron surface, for instance, fast etching and desorption of inhibitors and decomposition and/or rearrangement of the said inhibitors [29].

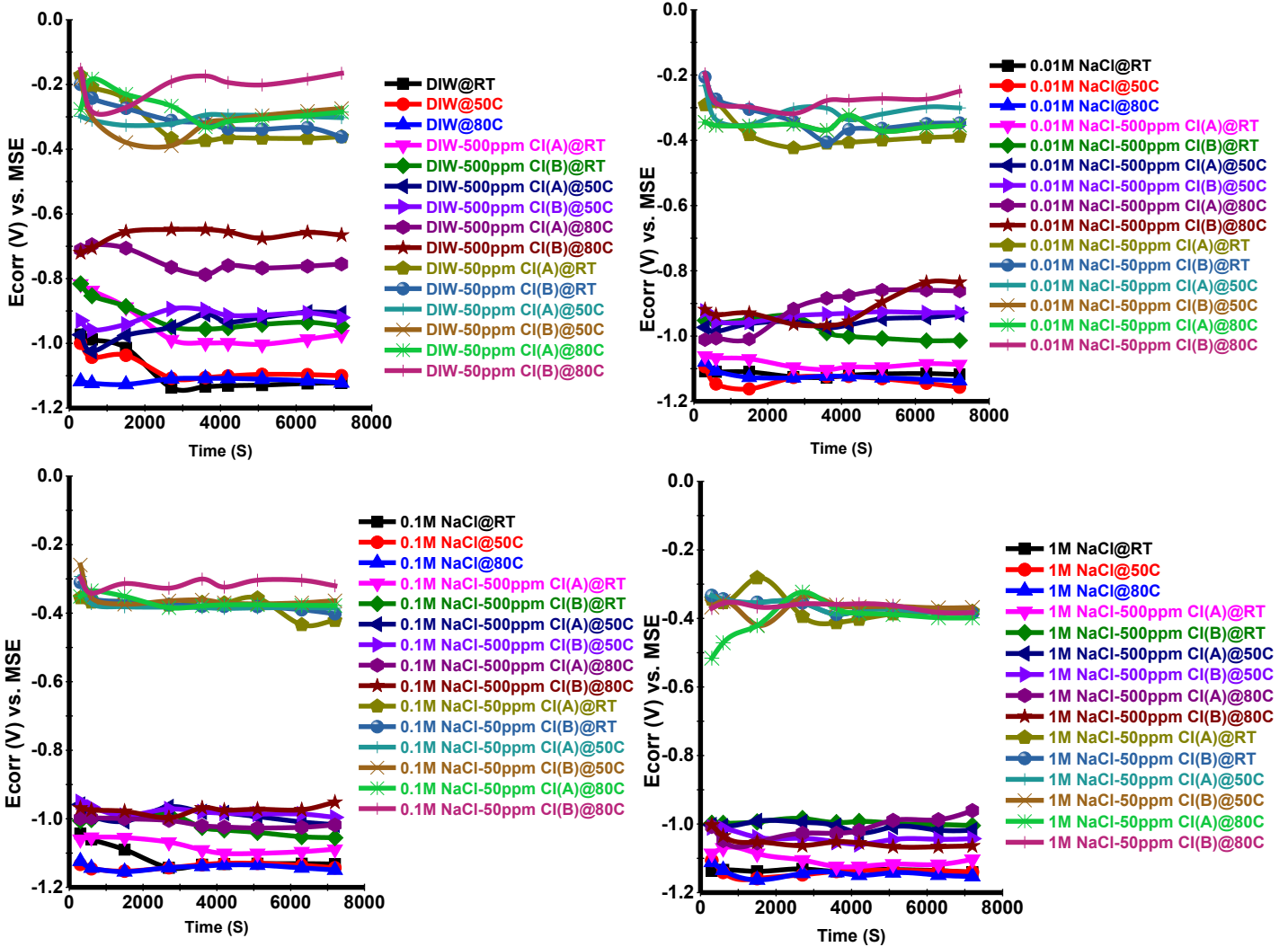


Figure 7. Variation of E_{corr} with time in different temperatures for DIW and NaCl with and without adding Cls in the H_2S system

Stage 1: Adding the Cl at the beginning of the reaction

Measurements of E_{corr} : The measurements of E_{corr} differences with time were vital to assessing the partial or complete inhibition and to determine the inhibitor threshold concentrations. The progression of E_{corr} of WE with time when altered amounts of the inhibitor were added is presented in Figure 7. The plots show a systemic trend with increasing the temperature resulted in more negative values for 500 ppm. It was also observed that inhibited solutions in RT with 500 ppm decreased and with the rise in temperature to 50°C for all solutions, and the E_{corr} increased and moved towards the positive potential values when the temperature was 80°C. The steady state E_{corr} value was achieved after about 1800 s of immersion for all solutions. In contrast, at 50 ppm in all temperatures, the E_{corr} pointedly grew within a few minutes, and a positive change was typically seen in E_{corr} of Cls on carbon steel in H_2S . This means there is a reduction in corrosion with temperature that could be recognised as the desorption of Cl increased on the surface. There was a movement towards positive values of E_{corr} in the existence of Cl in the system. This performance could be linked to changes in morphology and texture of the corrosion outcomes. Besides, there was a correlation between using the mixed type of inhibitor response and reduced corrosion and a suggestion of the functional behaviour of the protective films acting

to reduce corrosion.

Measurements of CR: As demonstrated in Figure 8, the corrosion rate rose with temperature in H_2S systems. This performance was possibly a result of the basis that rising temperature speeds up all the other signs of progress participating in corrosion, for example, electrochemical responses, chemical responses and transfer methods of the reactive sort to the metallic surface. In the occurrence of the inhibitor, CR was permanently much less than with the lack of the inhibitor. These consequences showed that the inhibitor was able at the variety of temperatures analyzed, and the lowest value for CR is at RT, then at 50°C and then at 80°C. The rise of the CR was particularly noticeable with the rise in temperature for a blank medium. In the existence of the inhibitor, the CR was hugely reduced at exploratory temperatures [30]. The temperature might impact the interface among the metal and the sour system both with and without the inhibitor. The CR for CS increased immediately with temperature in a blank solution. The decline of CR in the presence of the inhibitor mixture could be assigned to the chemisorption of the inhibitor on the surface, and the corrosion progression could link too many techniques of steel dissolution in the occurrence of the inhibitor. By raising the temperature, the inhibitor displayed inferior performance in the tests [9,31].

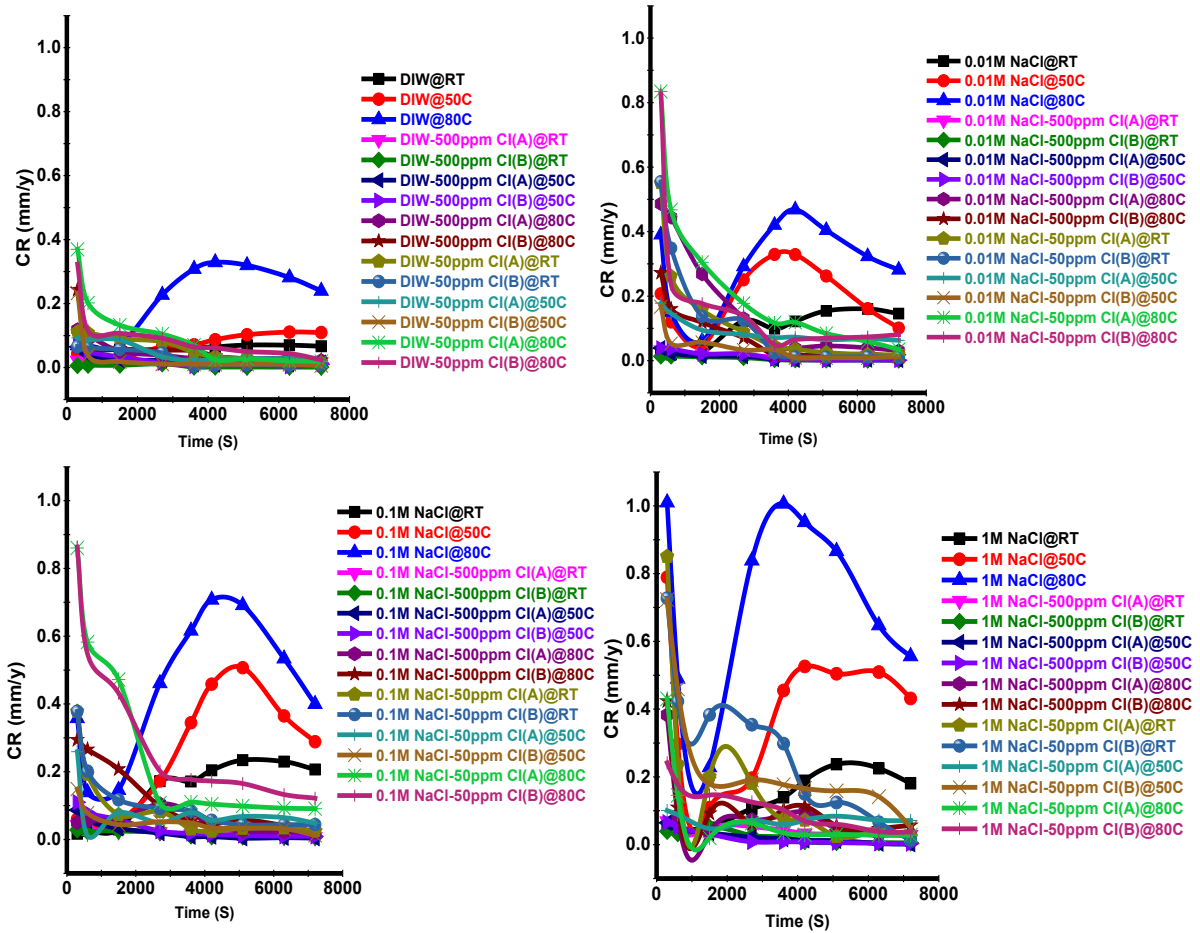


Figure 8. Variation of CR with time in different temperatures for DIW and NaCl with and without adding CIs in the H₂S system

Stage 2: Adding the CI after H₂S exposure

Measurements of E_{corr}: It can be noted from Figure 9 that the E_{corr} of the specimen at the beginning of the test when it was exposed to the H₂S environment only, moved towards even more negative values with time and stabilised around -1.15 V vs. MSE. After two hours of testing, there is a massive effect as the corrosion potential moved towards slightly more

positive values with time and with the addition of the CI and steadied around -0.4 to -0.3 V vs. MSE to end of the experiments. Those E_{corr} are inconsistent and different from the findings from stage 1 when CI is added at the beginning of the reaction. This might be credited to the build-up of a protecting CI film on the exposed surface of the specimen by adsorbing the inhibitor molecules on the surface. It shown has the inhibitor is affecting the surface even it added later.

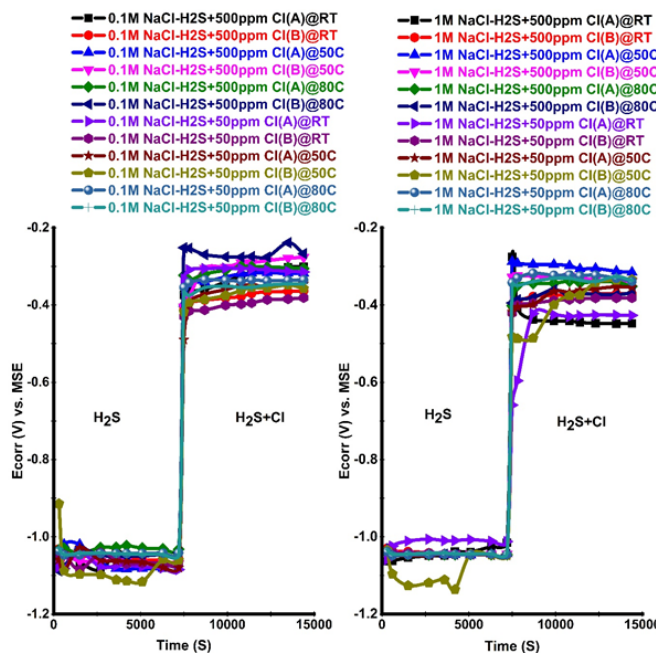


Figure 9. Evolution of the corrosion potential exposed to H₂S (2 hours), followed by adding CIs in H₂S (2 hours) at different temperatures

Measurements of CR: In Figure 10, the CR is calculated from I_{corr} results was high in the uninhibited solution with the coexistence of H_2S . H_2S molecules were adsorbed onto the metal surface and sped up its dissolution. Therefore, in these conditions, the iron sulfide layer that was formed was identically porous and let the aggressive ions to reach the alloys surface, so the CR was high. By adding Cls to the solution, the inhibitor particle was adsorbed by the steel surface and fell the I_{corr} , and accordingly, the CI is able

to access surface and inhibit. The rate of corrosion distinctly decreased after injecting Cls, and this significant decrease may be a consequence of the establishment of a protective layer, which is not fully covering the surface. There were significant modifications in the CR, measured throughout the rest of the test, through the working electrodes. They varied between 2 and 0.7 (mmpy).

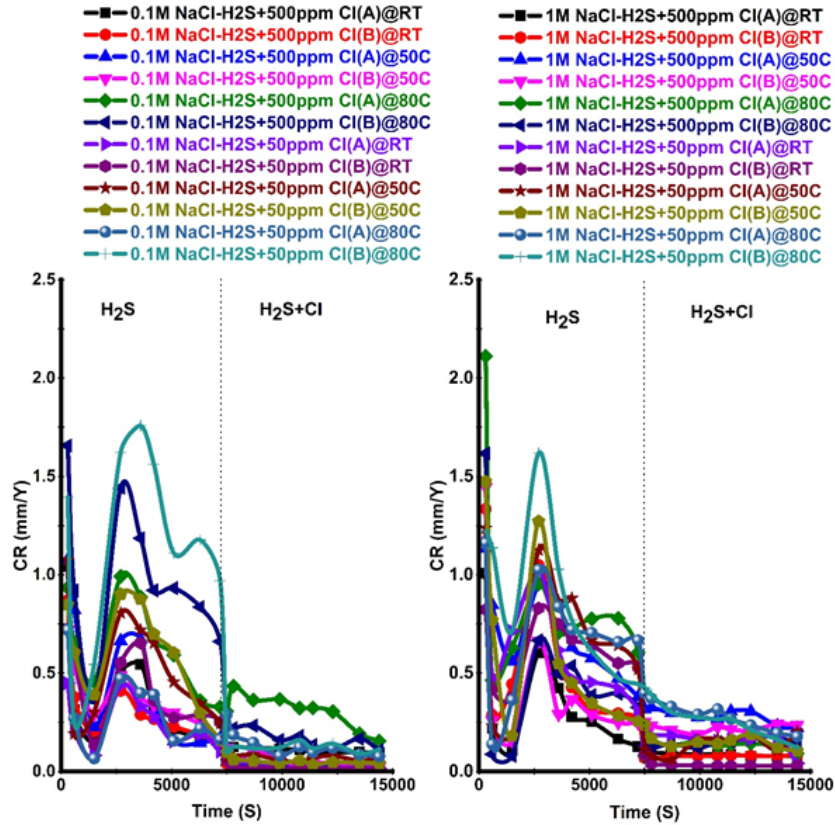


Figure 10. Evolution of the corrosion rate exposed to H_2S (2 hours), followed by adding Cls in H_2S (2 hours) at different temperatures

Furthermore, it appeared that a non-protective layer “FeS” was formed in the first two hours of the investigation for steels, which was defined by the rapid decrease in the polarization resistance. Nevertheless, the resistance increased after the introduction of the Cls. This corrosion reduction rate may possibly be assigned to the creation of a protective Cl film. All results are affected by Cl as required in industries as described in section 2. In the H_2S medium, the corrosion progression was mostly supplemented by the formation of FeS. The fact that E_{corr} raised initially and later, after a while, it declined because of the presence of a non-protective layer. The deposit was a non-adhesive layer that could be naturally extracted from a surface and could not passivate the surface under the conservational situations used here. The adhesion of the Cl film ought to have been influenced by other factors such as the adhesion and solidity of the inhibitor on this iron sulfide deposit. Once the inhibitor was injected, the CR declined; thus, Rp improved. So, by adding 500 ppm Cl, CR reached its min value, but at lower Cl concentrations, CR was higher than that achieved at 500 ppm. Conversely, similarly to the uninhibited solution, the CR of inhibited mixes rise over the period. Overall, it was recognised that Cl formed a protective deposit on the bare metal surface at high concentration Cl. Nevertheless, the reduction in the Rp amount in low Cl demonstrated that this layer inhibitor was uneven and unattached to the metal surface, as demonstrated in the SEM section. Furthermore, the metal was left unprotected and demonstrated a higher CR [32,33].

Inhibition Efficiency (IE%):

The difference in the inhibition efficiency (IE%), defined by LPR methods, was a function of concentration and temperatures. The efficiency was calculated based on

$$IE\% = \frac{I_{corr} - I_{corr (inh)}}{I_{corr}} \times 100$$

Based on percentage inhibition efficiency (IE%), Cls can be assembled into three categories: poor (when IE% <40); moderate (when IE% between 40 and 69); and excellent inhibitors (when IE% >70) [7]. The influence of salt concentration, Cls concentration, and temperature could be described with regards to IE% as shown in and Tables 4 and 5 for both stages 1 and 2. These amounts changed when the concentrations of both types of Cls accomplished more significant surface coverage. The changes may have been attributable to the statistical probabilities of electrochemical approaches resulting in instantaneous CRs. These differences might also rise in the time necessary to create an adsorbed layer of inhibitors on the metal surface that can impede corrosion [9]. The findings showed the dominant corrosion inhibition impact of examined corrosion inhibitors on corrosion of Iron in water and NaCl solutions. The utilization of a mixture of Cls with their best concentration exhibited a synergistic effect [34]. IE% was monitored for chloride ions concentration at various temperatures, and inhibitor concentration as those have affected the performance of both Cls for each stage (1 and 2).

Temp / Salt %	IE%					
	500 ppm-Cl(A)-Stage 1			50 ppm-Cl(A)- Stage 1		
	RT	50°C	80°C	RT	50°C	80°C
0	96	87	91	79	90	92
0.01	96	93	89	88	98	88
0.1	97	95	79	88	99	77
1	84	96	90	88	99	90
Temp / Salt %	IE%					
	500 ppm-Cl(B)-Stage 1			50 ppm-Cl(B)- Stage 1		
	RT	50°C	80°C	RT	50°C	80°C
0	97	86	91	87	94	96
0.01	99	99	96	93	87	71
0.1	97	97	94	79	96	70
1	97	99	95	92	88	93

Table 4. Inhibition efficiency (IE%) of CS in DIW and salt medium having different concentrations of Cls at various temperatures for Stage 1

Temp / Salt %	IE%					
	H2S+500 ppm-Cl(A)-Stage 2			H2S+50 ppm-Cl(A)-Stage 2		
	RT	50°C	80°C	RT	50°C	80°C
0	0	0	0	0	0	0
0.01	0	0	0	0	0	0
0.1	71	85	85	31	53	53
1	62	87	42	40	85	73
Temp / Salt %	IE%					
	H2S+500 ppm-Cl(B)-Stage 2			H2S+50 ppm-Cl(B)-Stage 2		
	RT	50°C	80°C	RT	50°C	80°C
0	0	0	0	0	0	0
0.01	0	0	0	0	0	0
0.1	87	94	82	74	84	88
1	69	90	51	59	57	72

Table 5. Inhibition efficiency (IE%) of CS in DIW and salt medium having different concentrations of Cls at various temperatures for Stage 1

Cl Concentration influence: It is obvious that the inhibition effectiveness in stage 1 (adding the Cl from the beginning of the tests) increases with added different concentrations to the test solution. The values of IE% for two inhibitors are given in both table and demonstrated that efficiency increased with rising Cls concentration. The outcome revealed that the Cls particles were adsorbed on the CS surface and created a protective sheet in both low and high concentrations. Significantly, the inhibition efficiency for both Cls is reached 97%. These results tell that the combinations of Cls under examination are reasonably efficient inhibitors for CS dissolution all solution. The inhibition of the corrosion of CS can be described in conditions of adsorption on the alloy surface [35].

Moreover, it has been noticed that the addition of this component tried to inhibit the acid corrosion of the iron at all concentrations utilized in stage 2 (middle of reaction after the corrosion product appeared). It has also been detected that a synergistic impact and improve the corrosion inhibition efficiency with concentration rise. The optimum concentration for highest effectiveness was noticed to be 500 ppm, where the efficiency reaches around 85% to 94% for both Cls. An additional increase in inhibitor

concentration substantially changes the protective effect. Such remarkable accomplishments, maybe because of the high molecular weight of the inhibitor, as well the inhibitor isolates the metal from the solution [35]. A synergistic effect that happened through the amount of Cl molecules adsorbed on the shell of iron is enhanced, produce adsorption film or a denser protective layer obstruct the mass transfer and charge transfer process on the iron surface.

Impact of temperatures

In general, EI% decreased with the experimental temperature. For both stages, inhibition efficiencies and have variations reading with increasing temperature. Such as the inhibition efficiency of (A and B) in all solution rises with rise in temperature up to at 50°C and beyond this decrease in efficiency was noted, that shows the stability of the adsorbed layer at the considered temperatures and is maybe caused by physisorption of an inhibitor particle adsorbed at less temperature, that is altered to chemisorptions at higher temperature [36]. With a further rise in temperature, IE% declines. This is owing to the instability of the adsorbed layer over 50°C. The rise in temperature moves the equilibrium in favour of the desorption method

than the adsorption route. So, a reduce in inhibition efficiency with a rise in temperature is called physical adsorption [6].

Effect of Cl⁻ ions

Moreover, with rising the ions of chloride on the solution, the inhibition efficiency decreased with the growth of temperature and the concentration of Cl⁻, showing that higher temperature dissolution of CS leads to adsorption of Cl⁻ molecules at the alloy surface [27]. The most significant inhibition efficiency of Cl⁻ (B) at 50°C. Therefore, it is remarked that the efficiency levels for (inhibitor A and B) presented higher values in DIW solutions and salts, which showed excellent surface coverage for rough surfaces. On the other hand, IE% of inhibitor (B) on the rough sample in salts solution suggested better Cl⁻ adsorption on the iron and thus resulted in greater surface coverage. It was evident that inhibitor (B) was a more efficient corrosion inhibitor than the inhibitor (A). The effectiveness count depended on the temperature and concentrations. Generally, IE% grew with the inhibitor concentration, and the value of all IE% in stage 1 is >70, and in stage 2 is >30.

From that all, in acid solution, corrosion of metal was attended by the release of H₂S gas. The growth in temperature accelerated CR, that led to a greater rate of metal dissolution. Data shows that IE% rises with temperature capable of 50°C, which defines the strength of the adsorbed film (adhesive coverage). The proliferation in IE% may be caused by the physically adsorbed combination that could be integral to the chemical interface of the steel. Through a further rise in temperature IE% drops. This is because of the variability of the adsorbed film over 50°C. The rise in temperature changes the equilibrium in favour of the desorption action rather than the adsorption process. Therefore, IE% falls considerably with the increase in temperature for both types of Cl⁻. The low IE% at high temperature is possibly caused by the vital movement of Cl⁻ molecules in the medium and on the metal interfaces in an acidic medium. The highly mobile molecule could be unable to adsorb onto the surface. It may be unsuccessful in forming coordinated bonds between the interfaces of the iron and the medium to form a barrier layer [14]. Moreover, IE% rose with an increase in the number of Cl⁻. This action may be assigned to the growth of the surface sections shielded by the adsorbed particles of Cl⁻. It is customarily supposed that the adsorption of the Cl⁻ at the alloy/medium interface is the primary phase in the mechanism of inhibition in destructive solution [30]. The results briefly define the reliance of elevated temperature on IE%. A study by Abdul et al. [6] indicated that IEs depends on temperature. They recommended that a rise up in temperature may trigger a fall in the ability of the adsorption route. This clarified the unflavoured adsorption situation at high temperatures and the drop in IE% amounts. The decline in the adsorption process described the physical adsorption approach. At high heat, the inhibitor particles in the sour media changed dynamically. Accordingly, the inhibitor molecules were incapable of adsorbing onto the iron surface because of constant collisions with all types of ionic particles in the solution. It can be summarised that the existence of Cl⁻ in the acidic media produces growth in the potential of the anodic and cathodic parts and decreases the I_{corr} . These fluctuations are increased by raising the amounts of Cl⁻, and this behaviour specifies the Cl⁻ adsorption on the surface of the metal and the shielding influence of the transfer of electrical charges and ions in the anodic and cathodic responses [37]. It is noticed that as the salt's concentration increases, the IE% also rises. At risen amounts, the interaction among the Cl⁻ molecules and the iron specimen would increase, thereby guiding to better safety of the specimen. The range of temperatures was from RT to 80°C, and the outcomes achieved showed that the amounts of Cl⁻ fell with rising temperatures. At a higher temperature, a decrease in IE% probably due to there was desorption of the adsorbed particles of Cl⁻, leading to the exposure area in the acid atmosphere to increase in CR and a decrease in IE%. Generally, IE% of Cl⁻ decreases at high temperatures of more than 50°C. Fast etching, desorption, and decomposition or reordering of inhibitor particles are some of the processes that decline the inhibition efficiency [14,38].

Surface morphology and structure of corrosion product films

SEM micrographs were referred to in order to establish a link between the experimental considerations and the morphology of the iron surface. The surfaces of CS specimens were taken at an identical magnification to observe the variations that happened through the corrosion progression and element distribution analysis.

Stage 1: Adding the Cl⁻ at The Beginning of The Reaction: Figure 11 characterised the surface image of the roughened specimen after immersion in the control solution without H₂S in the system for 2 hours in all temperatures. The surface of the CS samples after electrochemical control research was mostly clean with individual signs of a few visible pits on some of the specimen surfaces and fine, coarse crystal grains shown on the surface were made up of the main products of Cl⁻ ions according to the analysed composition of the scale. EDS images and chemical composition analysis results showed iron, carbon, and oxygen and chloride elements in the product layer on the C-steel surface. By raising the temperature, the pits, and the number of fine, coarse crystal grains of Cl⁻ with different shapes on the carbon steel surface increased. It showed up as salt crystal formation that even not removes with washing the sample.

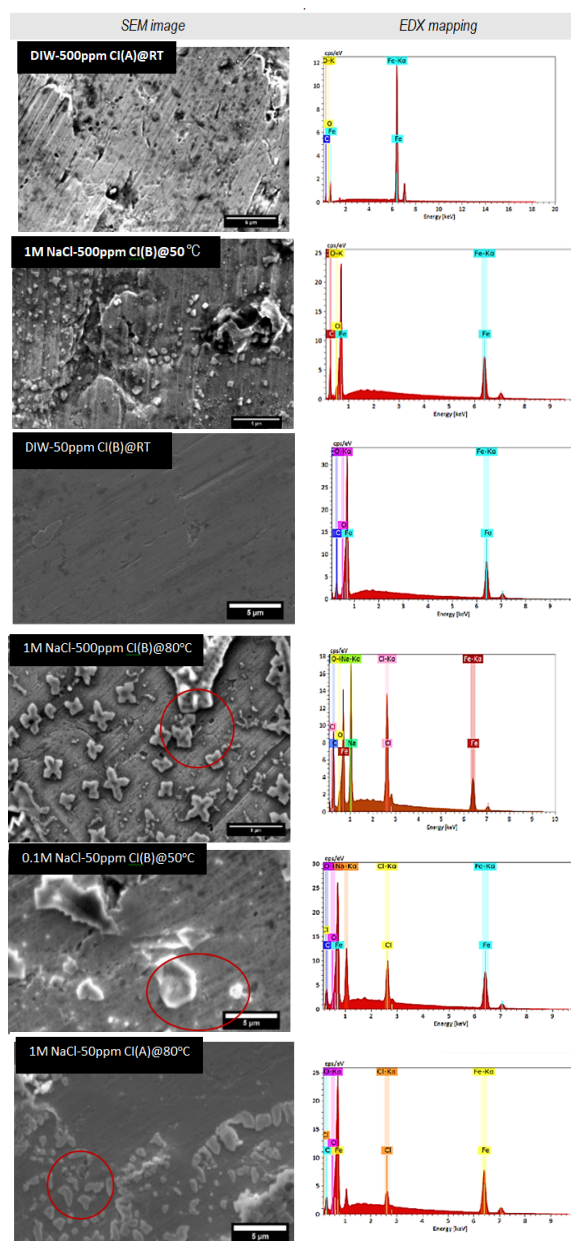


Figure 11. The morphology of the control solution tests (DIW and salts) with

adding Cls for OCP tests for 2 hrs. at a different temperature, Elemental maps for Fe, O, Cl⁻ and C

The micrograph of the CS surface in the existence of Cl under the OCP test is shown in Figure 12, which illustrated a considerable amount of space free of deterioration (un covered surface), scale products, and no pits or cracks; hence, the number of fine, coarse crystal grains disappeared in a higher concentration of Cls in all solutions of NaCl. By decreasing the number of Cls to 50 ppm, the existence of very rare corrosion products was detected with minimised pits or cracks in all NaCl solutions except the 1 M NaCl that showed no corrosion scales; however, salt crystal appeared, this is a most likely molecular template. By raising the temperature, a dense layer of corrosion products was generated with salt crystals. Element's analysis reveals that the sulfur element in the product deposit on the steel surface decreased, and the chloride element increased. These consequences demonstrated that the existence of base inhibitors delayed the dissolution of the iron owing to the development of a protective sheet via the adsorption of Cl particles onto the planar surface that reduces the CR. Although the morphology corresponds to the rising temperature, some bright clusters on the surface, similar to flowers or lettuce leaf structures, formed. There was a uniform element formed on the surface and the clusters. The crystal grains were not only spread in precise geometrical figures, but they were also often and thickly arranged.

Figure 12. SEM micrographs of the iron surface after immersion in inhibitor solution after applied OCP test during 2 hrs at a different temperature, Elemental maps for Fe, O, S, Cl⁻ and C

Figure 13 shows micrographs and EDX spectrum of the specimen surfaces of iron from the LPR test. It is observed that no corrosion products accrued on the bare metal, and it is a reasonably flat surface with diminutive pits or cracks, inclusions, and bright clusters in the LPR test at 500 ppm Cls. Even after washed and rinsed the surface by deionised water under N₂ gas. The EDS examination showed the existence of Fe, C, O, and S elements. However, some elements formed the clusters/inclusions, and it is observed that the surfaces were extraordinarily rich in Cl⁻. With increased temperature, the morphology is very similar across the surface; there are some inclusions and bright clusters. The element distribution is quite uniform on the surface. These consequences indicate that an inhibitor could form a product film on the steel surface by adsorption. This film has a high level of protection performance on the steel surface, i.e., block Fe²⁺ dissolution and the present precipitation of FeS.

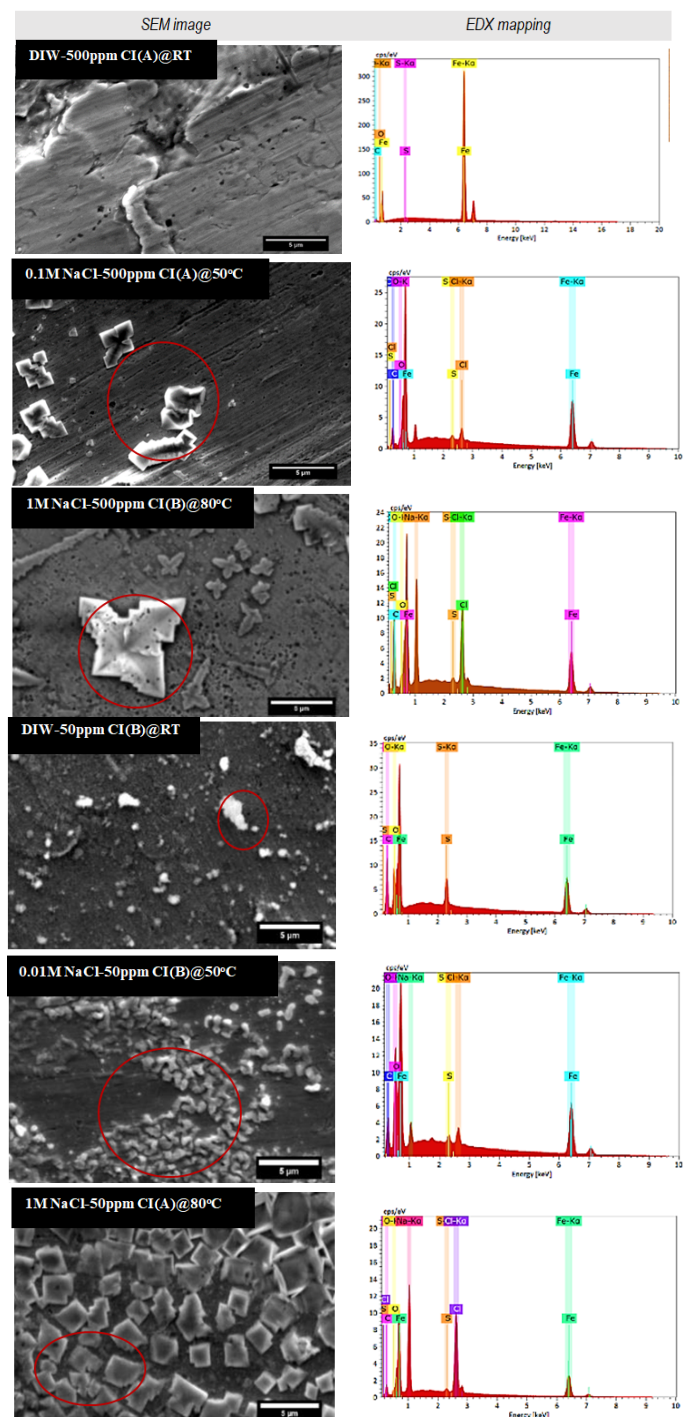
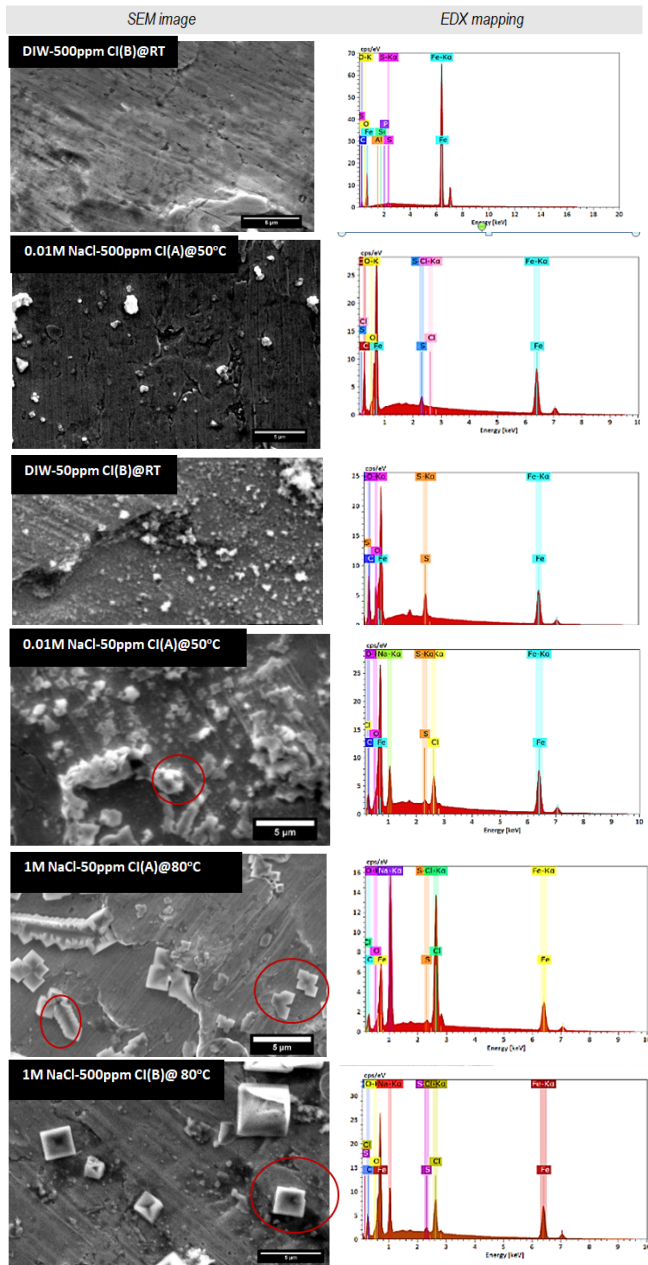


Figure 13. SEM micrographs of the iron surface after immersion in inhibitor solution after applied LPR test during 2 hrs at a different temperature, Elemental maps for Fe, O, S, Cl⁻ and C

It can be observed in Figure 14 from the PDP test that there are visible pitting and cavities on the bare metal surface and a corrosion product layer, which appears to be very dense. Some minor holes can be seen, and pits are deeper and more visibly noticeable on the iron surface. The marks on the surface are characteristic of corrosion products and the aggressive medium, even with the presence of inhibitors. This is mostly because of applied high voltage, which allows the coupon to release more iron into the solution, comment on localised corrosion as for not fully inhibited system [39]. Generally, the bare metal sample also displays appearances of uniform corrosion, and there is a lot of areas of peeling. The iron sulfide, i.e., mackinawite, is produced randomly with marked distances. In sour systems, however, it seemed that the inhibitors worked together with the formation of protective iron sulfide scales. This observation demonstrated that the CI worked through the creation of an insoluble barrier layer on the bare metal surface. Moreover, at low concentrations of CI, it resulted in a surface with fewer pits and fewer failures via the adsorption of the inhibitor. The photomicrograph showed the creation of a smooth, even deposit of the inhibitor (B) on the metal surface in solution NaCl more effectively than in DIW. This proved that the inhibitors prevented the corrosion of metal by adsorption on the bare metal surface. Inhibitor (A) was suitable for DIW, and (B) was suitable for NaCl solutions. Further investigations need to do to study the depth of the pits in carbon steel.

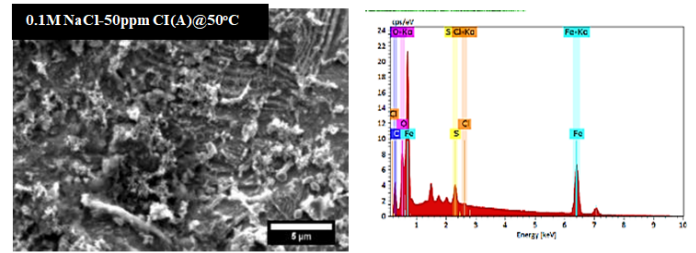
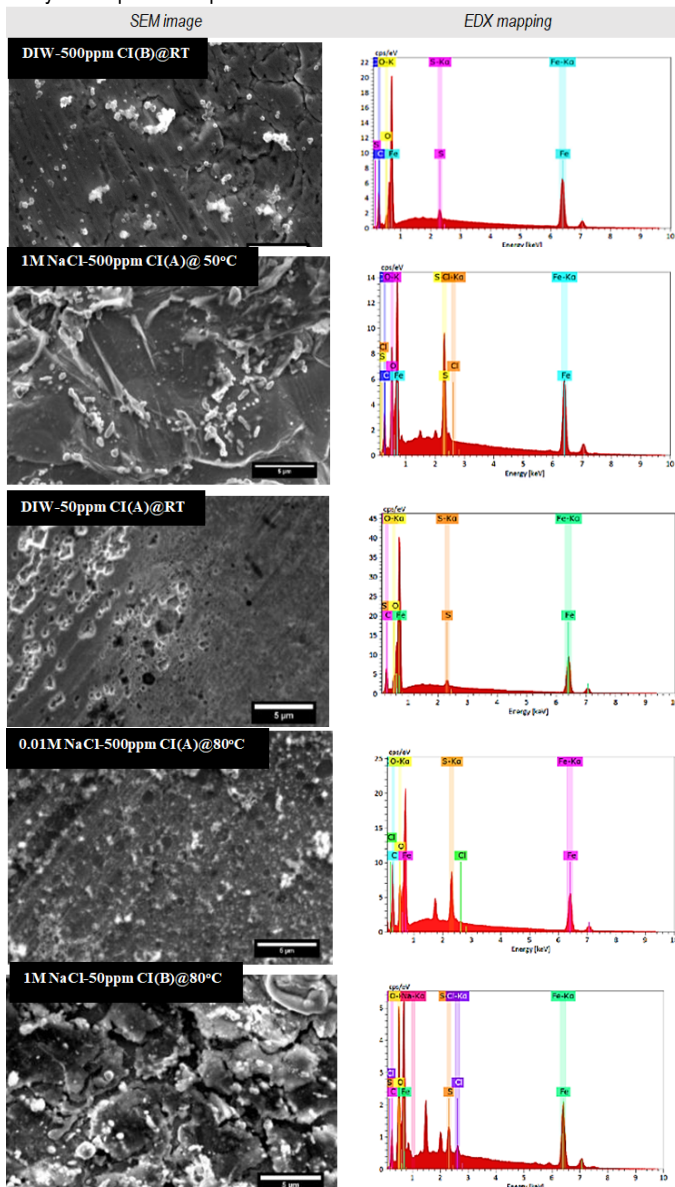
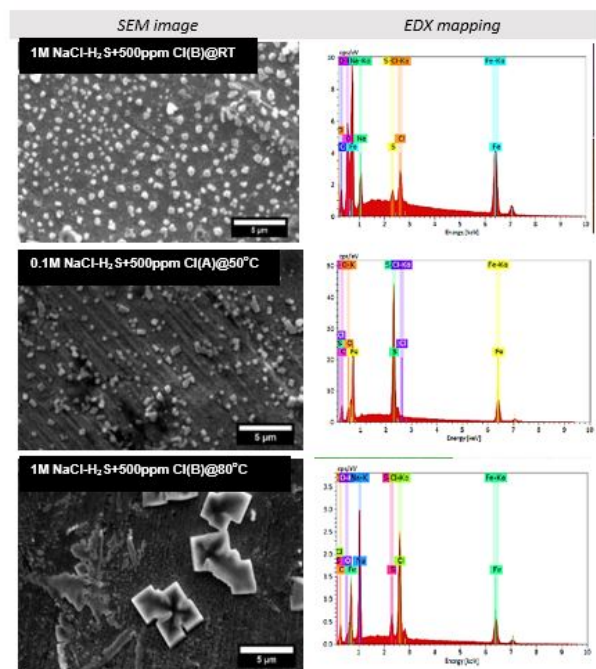


Figure 14. SEM micrographs of the iron surface after immersion in inhibitor solution after applied PDP test at a different temperature, Elemental maps for Fe, O, S, Cl⁻ and C

Stage 2: Adding the CI after H₂S exposure: The SEM image of corrosion films shaped in NaCl media saturated with H₂S after adding CIs for the extended falling period is revealed in Figure 15. It can be observed that the impact of CIs on the morphology of iron corrosion is outstanding. At the primary phase of the test, the corrosion layers were fragile and porous, resulting in poor safety. Ions of the media could radically extend the bare metal surface through a tinny and porous corrosion film with different soluble salts. Chlorides and sulfates were the main part of the corrosion layer, and most of them had crystalline salt, which was detected as different shapes, such as a single cubic particle, smaller salt particles, large central, and satellite salt particles, and clusters of salt particles. After four hours of immersion in the OCP test, it was evident that a film of corrosion products. These FeS layer forms were uneven, porous, and made up of asymmetrical crystal grains at lower concentrations of CI at room temperature. After increasing the concentration to 500 ppm CIs, the film contrasted with the corrosion layer at low CIs. It also had irregular crystal grains. This crystal was fine and loose and occurred in the corrosion film. With further increase of temperature, product deposits converted to thicker wispy yet still porous deposits, as shown in RT and the low concentrations. With the high amount of CI, the fine, irregular/regular, and bulky grains of corrosion films displayed slightly more density as the temperature increased. Consequently, it is evident that the bare metal corrosion surface that had the compressed and continuous grains present on it, which might block the destructive ions present above the film, was better protected against the sour environment [18]. Those salts crystal might be formed during the process, and the sample was extremely washed and rinsed with distilled water and dried with N₂ gas, but these crystals were not removed. Also, the appearance of salt crystals covered the surfaces of the real protective layer, and subsequently, the CIs hampered the growth of FeS and appeared under the salt crystals.



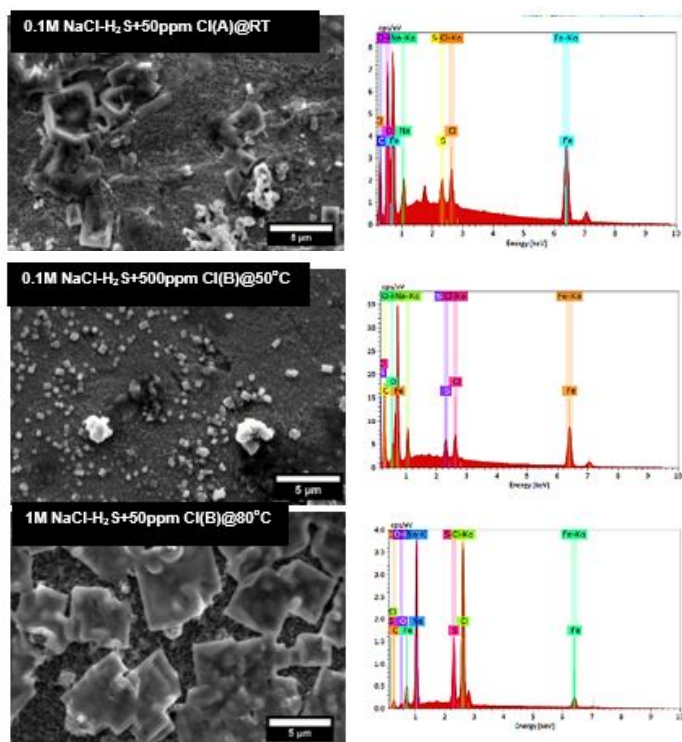


Figure 15. The SEM micrographs of the corrosion products layer generated on the OCP test in step two, Elemental maps for Fe, O, S, Cl⁻ and C

The SEM pictures from the LPR experiment of the corrosion products layers produced under the different concentrations of salts, Cls, and temperatures can be seen in Figure 16. The compact and impeccable rust products covered coarse and porous features with small cavities in RT. With rising temperatures and increasing with the amount of Cls, the product was thicker in contrast to the deposit generated using big porosities and coarse grains; it was more dense and opaque than that are at RT. That means that the scale of FeS formed under the crystal particles was very big and bulky and not compact. Furthermore, the shape of many crystal grains that were found was seen to be irregular, on many porous layers, and stage lines could be discovered under them. Large holes with some cracks and minor pores additionally existed between and under the crystal grains [40]. As a result, corrosion product layers included large crystal grains bonded together, and consequently, the films were porous. Based on the electrochemistry data, it is clear that Cls can enter FeS film and react with the metal and might be placed in the apertures of the corrosion films. Therefore, the corrosion product deposits became denser. Also, it is clear that increased numbers of Cl⁻ ions created intermediate corrosion types [40]. Salts crystals (NaCl) were noticed in all tests that form in the solution, which showed that even the washing process did not eliminate all the salt accumulated. The crystalline NaCl extant in the FeS layer through the corrosion progression remained [41]. EDX results showed that at RT with low salt values such as 0.1 M and low Cls concentration of 50 ppm, only iron sulfides were detected. With the rise of Cls concentration to 500 ppm, the Fe peak was significantly reduced, which specified a strong adherent protective layer with a crystal NaCl cover film with the presence of FeS. As the Cl ion exist in the protected layer as in the solution Cls. The relative intensity of the analysis of the peak of the salt's ions increased with the increasing Cls, salt concentration, and temperature. This observation was impartial of the solution value of temperature and the concentration of Cls. The composition of corrosion product layers generated on both tests was made of Fe with crystalline iron sulfides; salts were also detected. Plotting the data displayed a higher concentration of Cl ions than Na ions in the centre of the surface area than on the outer layer, suggests constructs of Cl and species. This confirmed that different types of crystal structures appeared on the surface, and the Cl⁻ is incorporated into the surface and just present as electrolyte residue.

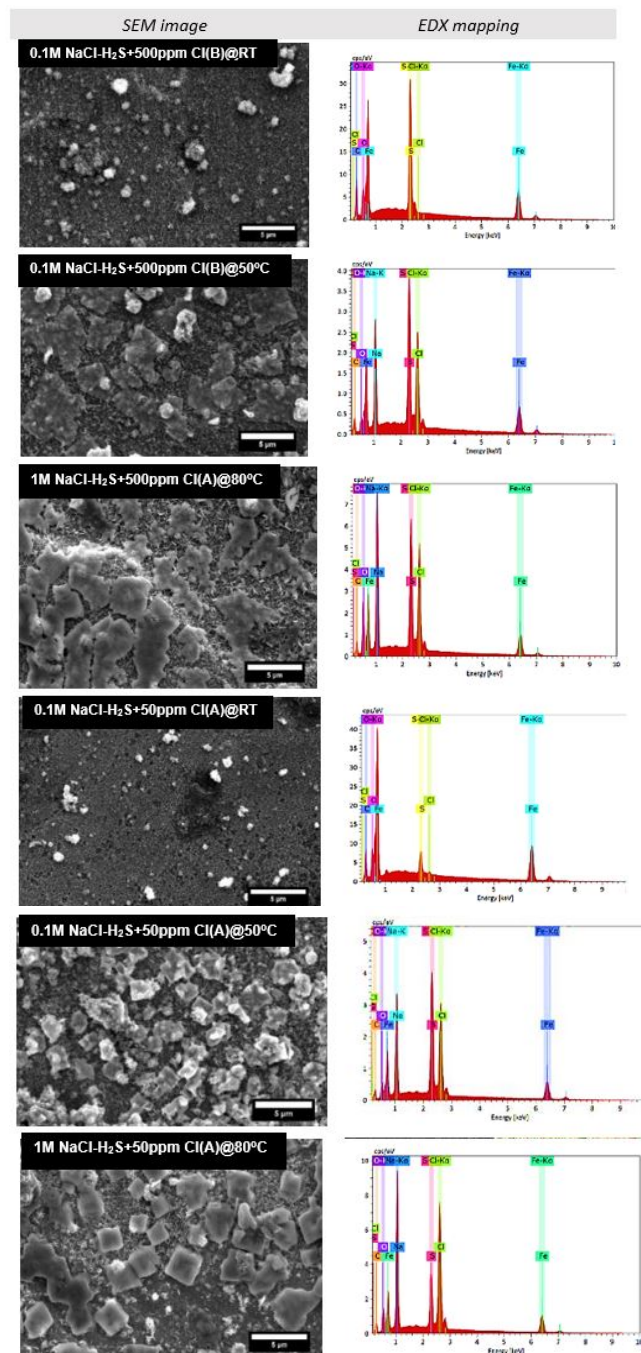


Figure 16. The SEM micrographs of the corrosion products layer generated on the LPR test in step two, elemental maps for Fe, O, S, Cl⁻ and C

Raman Analysis (RA) of corrosion product

Ex situ Raman spectra are very strong when used to examine and characterise the structure of protective film on the steel surface and predict the types of bonds that may occur. Raman arrays were achieved after the formation of corrosion layers on the bare metal by EC testing for stages 1 and 2. All specimens analysed using Raman spectroscopy showed three regions of different colours. Three spectra were obtained for each of these regions in three different areas: at the centre and at each border.

Stage 1: Adding the Cl at the beginning of the reaction: The RA spectra of control solutions and corrosion products of steel dipped in 500 ppm and 50 ppm inhibitors are depicted in Figure 17 were scanned in the air. For Raman spectra in the vacuum of control experiments and 500 ppm, Cls

inhibitors at different temperatures for step 1 in OCP and LPR test showed there was no variation, no broadband in the region of 200-1400 cm^{-1} . This definite the occurrence of adsorbed inhibitors on the steel surface. The corresponding Raman spectrum (Figures 18 and 19) in 50 ppm shows three peaks at 219, 285, and 690 cm^{-1} , which is a broad, less intense band of the spectrum. Similar spectra were already reported and attributed to "amorphous" or "poorly crystallised" FeS, identified as corrosion products of steel, appeared on a surface with the presence of goethite (alpha FeOOH). The virtual intensity of the peaks suggested a mackinawite rise with the increasing temperatures and concentrations of salt and Cls. Figure

20 shows only a few weak bands appeared for iron in chloride solutions. The bands at 219, 285, 395, and 590 cm^{-1} have been stated to be owing to the dissolution into ferrous and ferric cations, which results in and are produced by the corrosion processes [42]. Raman patterns took on the creation of corrosion films on the steel by potentiodynamic processes in an acidic solution that mixed with Cls. Overall, it can be noticed that the occurrence of similar peaks via both approaches demonstrated the signs of different iron sulfide mixtures formed in different areas. Also noticeable was the presence of mackinawite, troilite, greigite, marcasite and pyrite and the rest for the iron oxides and goethite.

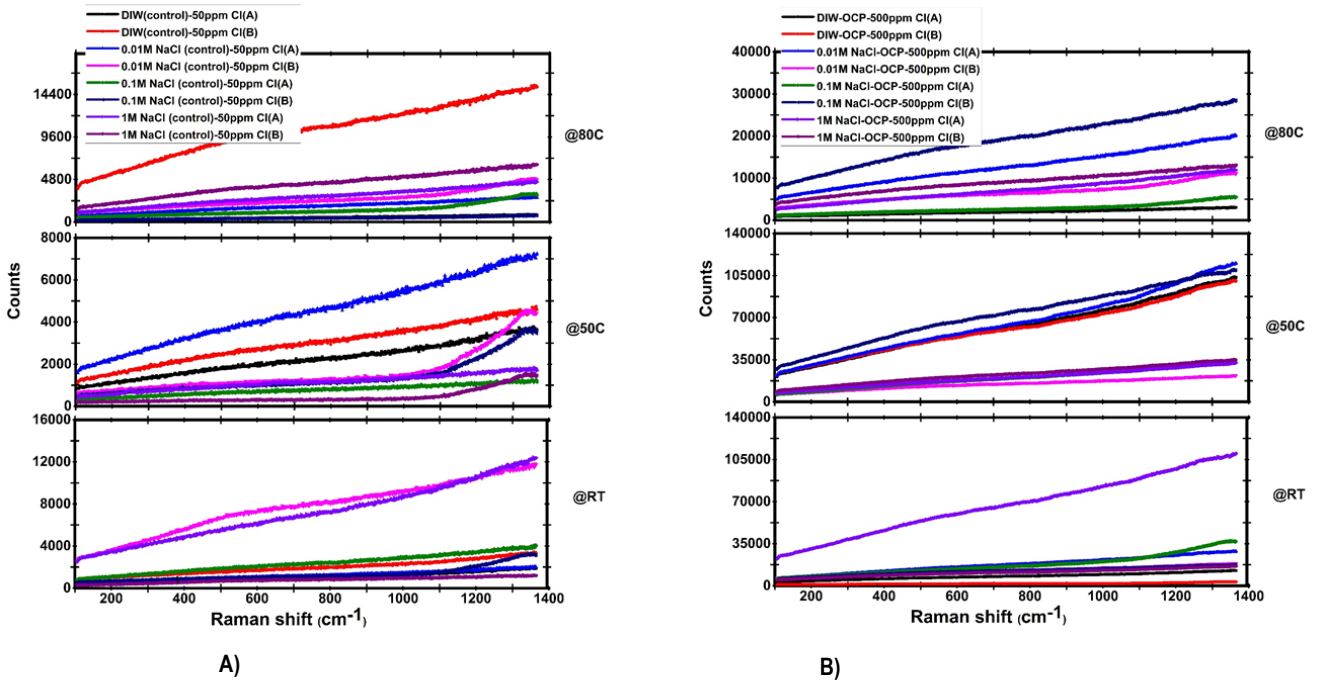


Figure 17. Spectra for control in different solution and temperatures for A) 500 ppm Cl and B) 50 ppm Cl

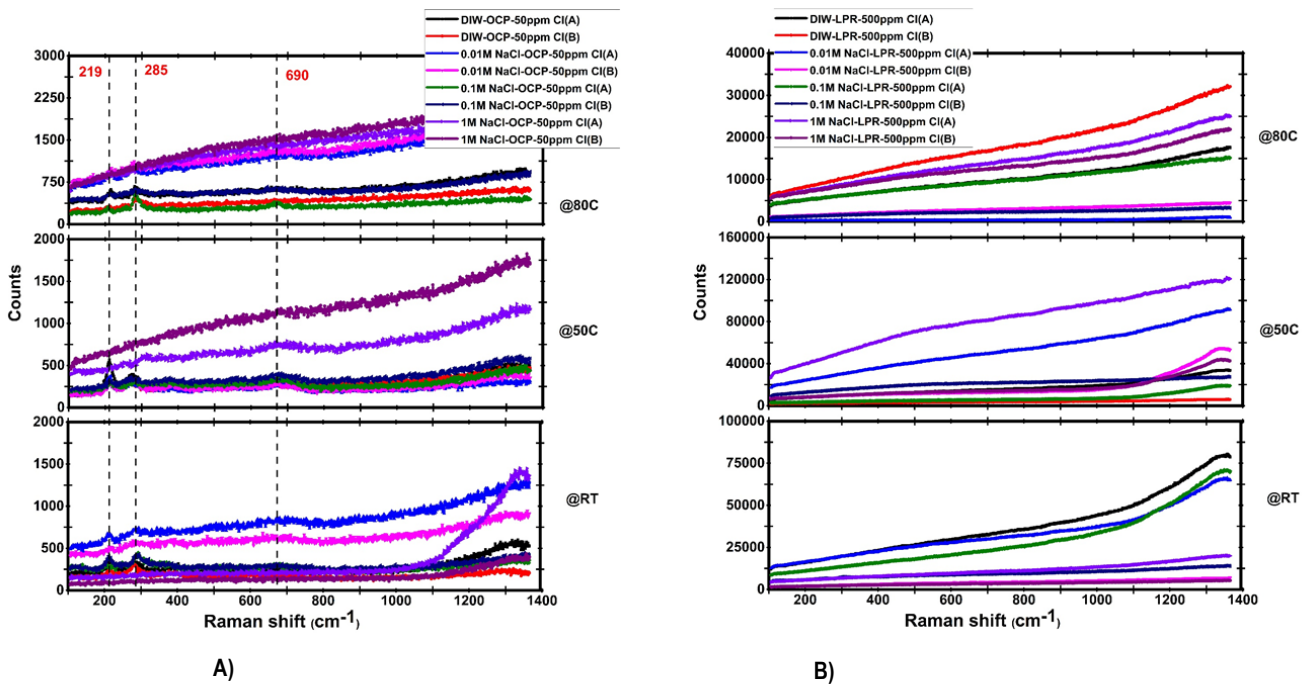


Figure 18. Spectra for control in different solution and temperatures for A) 500 ppm Cl and B) 50 ppm Cl

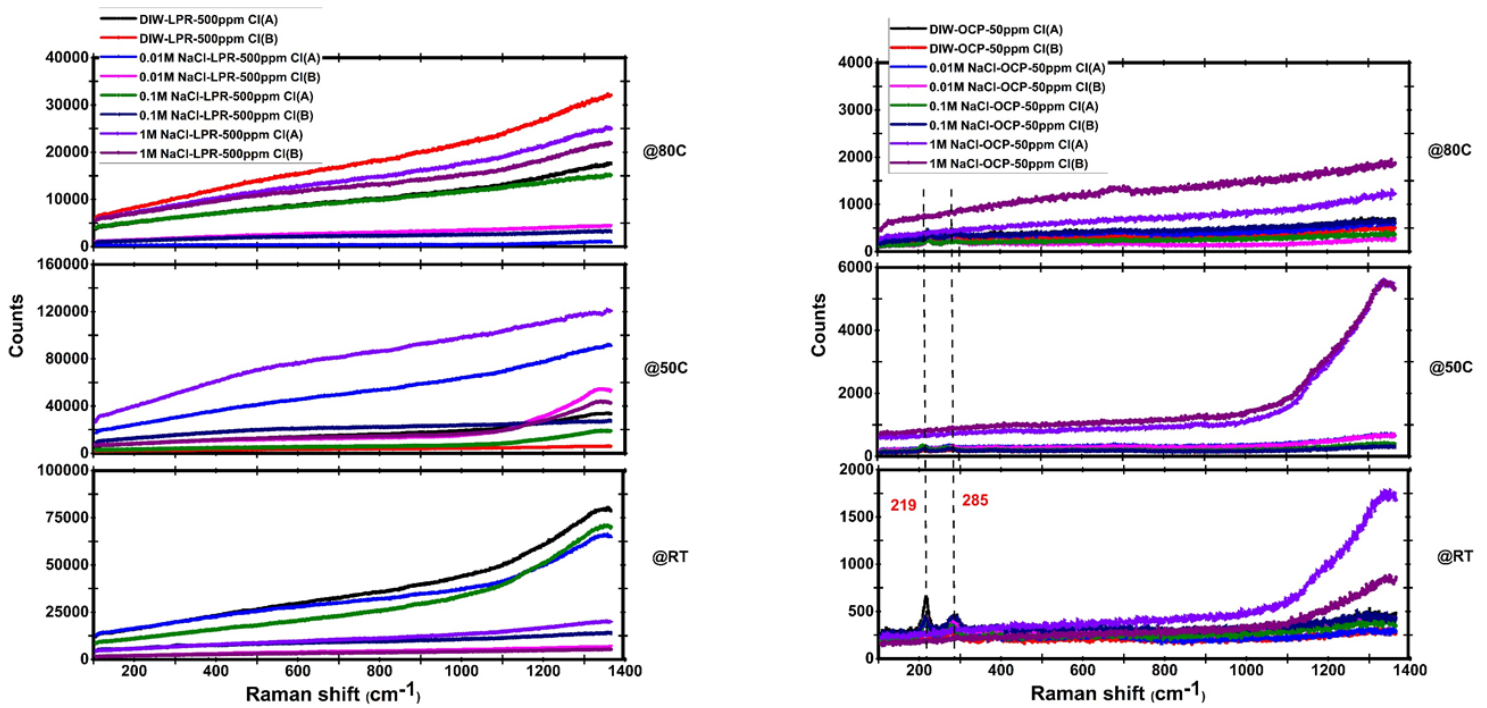


Figure 19. Raman spectra of the iron surface obtained after the LPR test for Stage 1 A) 500 ppm Cl and B) 50 ppm Cl

Stage 2: Adding the Cl after H₂S Exposure: In the range below 1000 cm⁻¹, both spectra revealed three individual Raman peaks with a broad shoulder, suggesting that the same mixtures were found along with all the corrosion progression. The spectra in Figure 21 are indicative of the numerous spectra that were found throughout the study of different spots on the metal surface and displayed an excellent arrangement on the spectra of the mackinawite as is discovered in nature. Nonetheless, the films electrochemically matured at stage 2, as shown by the creation of iron sulfide (FeS). It appears that the

OCP and LPR actions somewhat altered the chemical configuration of the sulfide films. It shows that FeS was the core corrosion product at various Cls contents. This result indicated that Cls did not affect the structure of the corrosion product. So, Cls does not affect film formation, and Cls are not integral to the corrosion reaction. However, Cls can still end up in the FeS films and alter the morphology of the corrosion layers in H₂S corrosion [8,28,43–51].

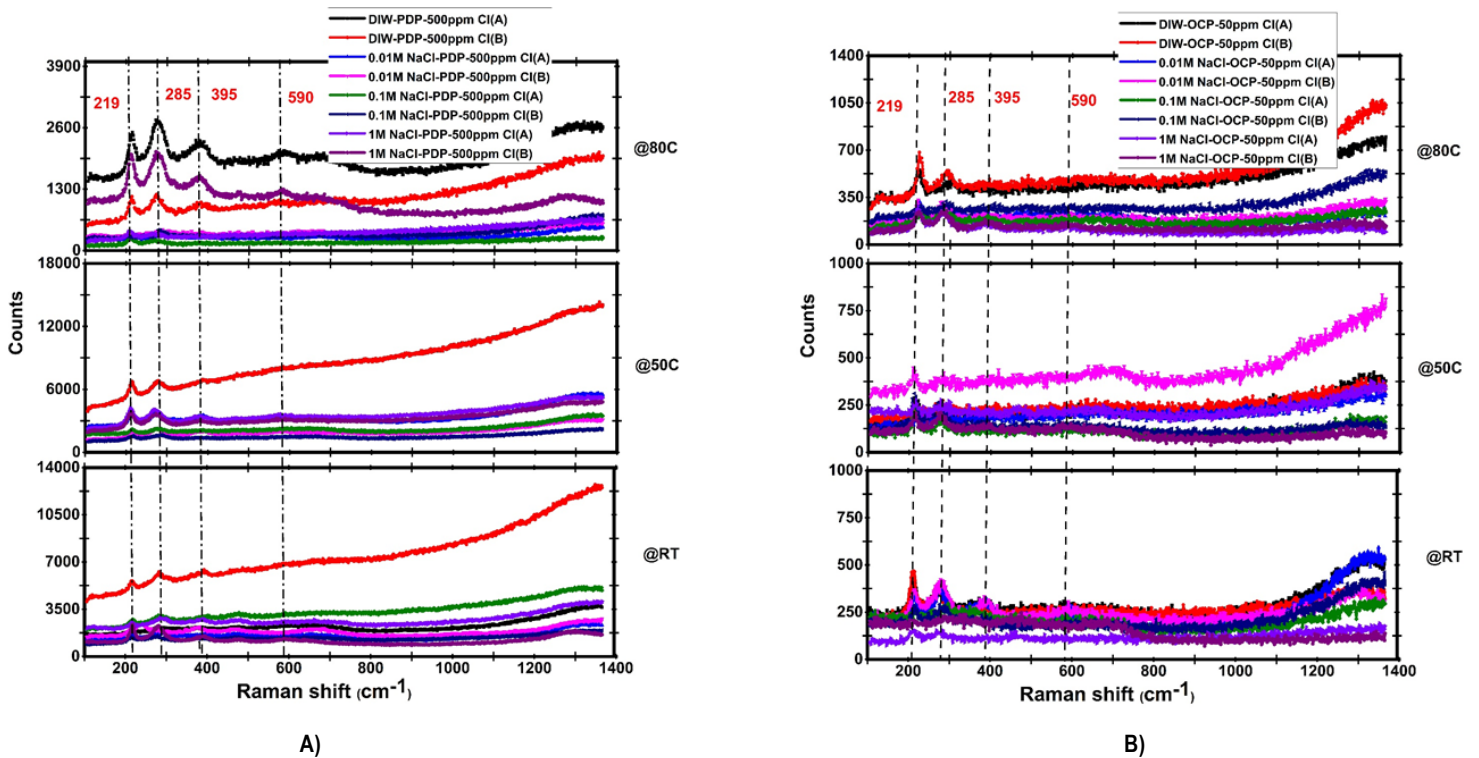


Figure 20. Raman spectra of the iron surface obtained after PDP test for Stage 1 A) 500 ppm Cl and B) 50 ppm Cl

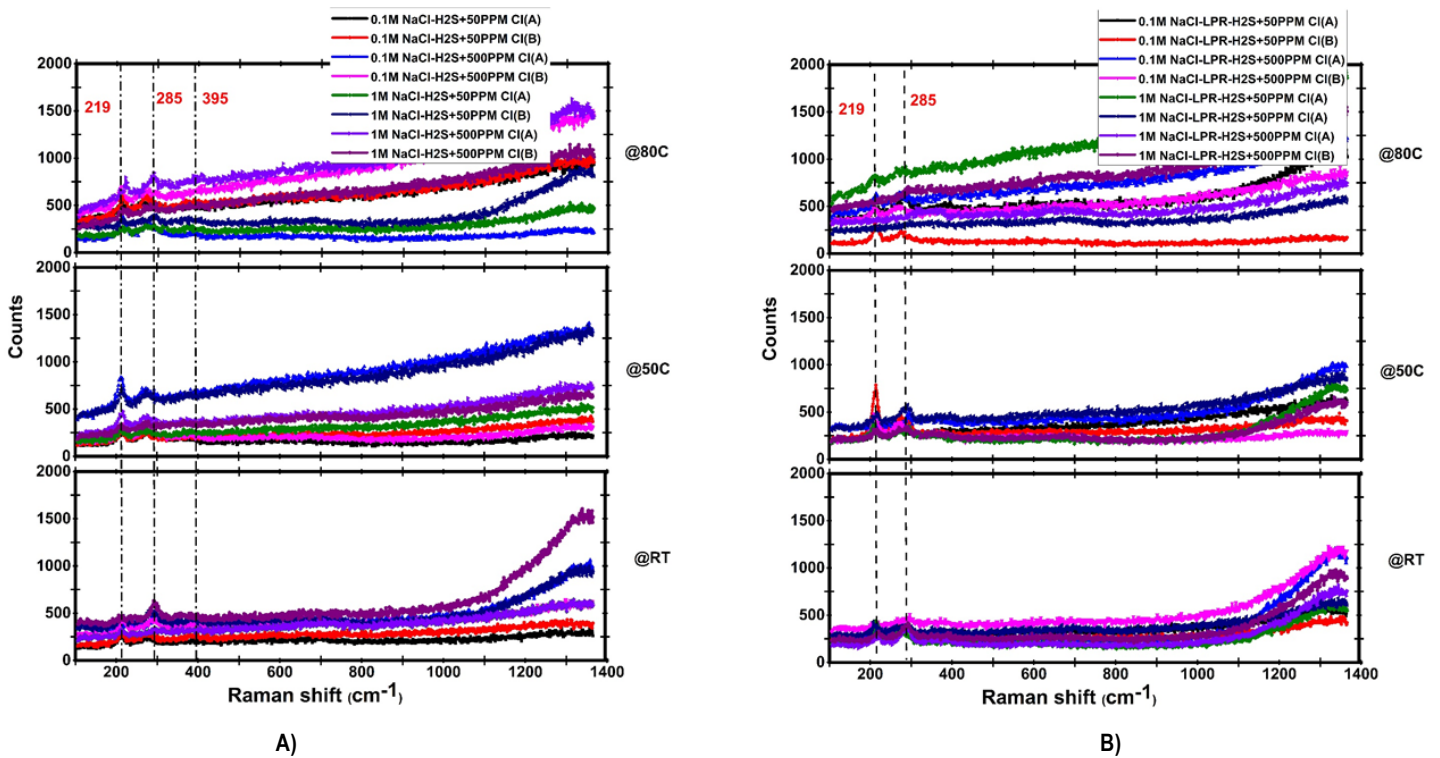


Figure 21. Evolution of the corrosion layer after exposed to H₂S (2 hrs), followed by adding Cls in H₂S (2 hours) at different temperatures for the A) OCP test and B) LPR test

Synergistic and antagonistic effects

Several mixtures of Cls combinations have similarly been highly examined in the earlier period in the formula of combinations of elements in addition to incorporated mixtures. In numerous situations, such compounds have been demonstrated to generate a synergistic influence. This synergy is suggested to be because of Cl mixtures not individual having both elements presented in medium, however precisely the existence of specific complexation and speciation (which means not only the distinct dissolved components) at the spots of corrosion that produces to an exclusive defensive layer. Such interaction, on the other hand, is not continuously applied in commercial circumstances, with many Cls having one effective ion and a simple counterion, and in such instances, the counterion is simply an observer, with no effective part [52]. Therefore the synergism and antagonism can be identified as if the inhibitor adsorption raises and improves the protective influence of the film is synergism or else, on the opposite, reduces it is antagonism, and then the valuation of these influences and contributions becomes more problematic. The occurrence of synergism and antagonism is only achievable with regard to the act of the inhibitor in the existence of a surface film with a non-air oxide nature [53]. The occurrence of synergism has also been established markedly in the water and chloride

containing media, and it has been displayed that inhibition implementation of several organic and inorganic inhibitors necessarily influenced by the attendance of external additives. The existence of inhibitors layer on the shell divides metals from the solutions and thus defends from corrosion. The existence of metallic cations improves the adsorption of these inhibitors during synergism [52]. Cls integrate into the deterioration product sheet and establish a defensive wall among the base alloy and the corrosive mixture. It is recommended that the composition of the Cls should be applicable to cooperate with the deterioration results and that they be able to be efficient on FeS. To expect the adsorption process of inhibition onto alloy surface, deterioration behaviour of CS need be well known. According to the electrochemical reaction, steel corrosion includes transfer of dual electrons, and then there are two actions where everyone symbolizes transfer of one electron and one of them might be assumed the rate determining stage. This consequence is in good quality arrangement with the processes that are proposed for iron dissolution in as follows Table 6 [54]. The species (FeOH)_{ads} and (FeClOH)_{ads} are the adsorbed in between and rate determining step is involved in steel dissolution as stated by the mechanism. Furthermore, the occurrence of Cl⁻ ions does not eliminate dissolution during the (FeOH)_{ads} intermediate in chloride free acid solutions, as the two processes can carry on concurrently [44,52,53].

Type of media	Reactions of the system
Aqueous solutions	$\text{Fe} + \text{H}_2\text{O} \Rightarrow [\text{FeOH}]_{\text{ads}} + \text{H}^+ + \text{e}^{-2}$ $[\text{FeOH}]_{\text{ads}} \Rightarrow [\text{FeOH}]_{\text{ads}}^+ + \text{e}_{\text{ads}}^-$ $[\text{FeOH}]_{\text{ads}}^+ + \text{H}^+ \Rightarrow \text{Fe}^{2+} + \text{H}_2\text{O}$
Aqueous solutions containing Cl ⁻ ions	$\text{Fe} + \text{H}_2\text{O} + \text{Cl}^- \Rightarrow [\text{FeClOH}]_{\text{ads}}^- + \text{H}^+ + \text{e}^{-2}$ $[\text{FeClOH}]_{\text{ads}}^- \Rightarrow [\text{FeClOH}]_{\text{ads}} + \text{e}_{\text{ads}}^-$ $[\text{FeClOH}]_{\text{ads}} + \text{H}^+ \Rightarrow \text{Fe}^{2+} + \text{H}_2\text{O}$

Table 6. Mechanism of alloys in different kinds of electrolytic media

In the sour system, Cls compounds can occur as protonated species (i.e., an atom, molecule, or ion). These varieties might adsorb on the cathodic positions of the steel surface and reduce the evolution of hydrogen. Also,

these combinations are capable of adsorbing on anodic spots through the type of an electron donating group, which affected on decline anodic dissolution of alloys [55]. There is a well surface covering on the CS surface

in the existence of CI that offers a good IE%. This is attributable to the participation of CI particles in the interface with the response spots of the CS surface, causing a decline in the interaction among the iron and the aggressive solution and it consecutively has shown outstanding inhibition impact [44,52,53,56]. Consequently, A and B are commercially employed as corrosion inhibitors commonly in oil pipelines. The synthesis of such CIs that objective dual activity by integrating both anions and cations which have indicated support of effective inhibition in all solutions. It has been revealed that, under all conditions with a short term of experiments, substantially decreases the corrosion current density of the CS, with extreme inhibition efficiencies in DIW and chloride solutions. For each condition, nevertheless, different mechanisms of protection are occurring and indicating a strong synergy between two ionic species. For example, in NaCl media, the chloride ions initially adsorbed at the interface of steel/solution at the deterioration potential via electrostatic attraction force as a result of the extra positive charge at the steel/solution interface. This procedure modifies the amount of the media side of the interface from positive to negative, and therefore assisting physical adsorption of the CI cations. Therefore CI (A and B) cations are equipped to electrostatically adsorb on the steel surface hidden with primary adsorbed chloride ions. Chloride ions encourage the physical adsorption of CIs on the steel surface. Besides the physical adsorption, there must be chemical adsorption in consequence of the direct bonds created among the electron sets of the unprotonated atom and the vacant loops of iron atoms that improved the arrangement intensity in the middle of the CIs particles and electrode surface [56–59].

Conclusion

In the current investigation, by carrying out comprehensive experiments with assured concentrations and types of corrosion inhibitors, at a selection of temperatures, results showed that the inhibiting effect of two inhibitors, in particular, was obvious in all solutions. In tests with just one effective inhibitor, all samples expressly showed scale formation, and the various properties of the inhibitors became obvious. The subsequent conclusions were drawn from this study. The timing of the addition of the CI to the solution played a significant role in the corrosion within a hydrogen sulfide environment, prevent formed of FeS. All investigational specimens in a sour medium in the absence and presence of inhibitors with two distinct concentrations. The potential of the experiment was monitored as a function of time to survey the progression of the film chemistry as it fell to equilibrium with the solution. When CIs were added at the initiation of the reactions, the E_{ocp} values reduced at all temperatures to negative values with different concentrations of CIs. The characteristic behaviour of inhibitors acted in conjunction with the solution as a mixed kind of inhibitor and was adsorbed on the bare metal surface. Both types of inhibitors, A and B, worked by decreasing both the anodic and cathodic responses. Most surface images displayed a protected bare metal surface, which results from the adsorption of inhibitors onto it, and the decline of the CR. The value of CR of CS decreases as the concentration of CI (A and B) increases with regard to temperature. The presence of CI reduces the CR and I_{corr} conspicuously with a rise in the quantity of inhibitor linked with changing of corrosion potential (E_{corr}). The protection delivered by the inhibitor was limited, and the amount of protection declined with the low concentration of CI ions and in the rise up of the temperature. The inhibition efficiency of the inhibitor rose with the inhibitor amount, but it fell slightly with a rise in temperature. In the existence of CIs at a temperature of RT -50°C, ideal corrosion inhibition with good IE% resulted. At high temperatures, i.e. 80°C, the IE% decreased. Adding the CIs during the reaction, after the iron film was formed on the surface had different results. A free solution, the CR of CS, increases with time, which in turn indicates that more and more CS is lost by dissolution. However, when CIs are introduced in the solution, the absolute values of corrosion rate are low than those in the absence of CIs, indicating inhibition of CS corrosion. Exposure to the CI solution altered the film morphology. SEM images showed significant inhibition effect in the presence of A and B with higher CI concentrations compared to the corroded iron surface in the acids alone.

Outcomes showed that the most significant active CI commercial products; however, they were less efficient at higher temperatures. The value of IE% reduces with the rise in temperature. Thus, both CI (A and B) performs as a temperature dependent inhibitor and the correlation among temperature and inhibition efficiency is as well a characteristic of the physical adsorption.

Acknowledgements

The authors wish to thank Qatar Shell (QS), Shell Global Solutions, Advanced Interfacial Materials Science (AIMS), and Qatar University (QU) for continuous financial support and technical guidance led to this publication.

References

1. Kasnick, MA and Engen RJ. "Iron sulfide scaling and associated corrosion in saudi arabian khuff gas wells." *Middle East Oil Show* (1989).
2. Kvarekval, J and Dugstad A. "Pitting corrosion mechanisms on carbon steel in sour glycol/water mixtures." *NACE Meet Pap* (2004): 1–15.
3. Al-Sabagh, AM, Nasser NM, Khamis EA and Mahmoud T. "Synthesis of non-ionic surfactants based on alkylene diamine and evaluation of their corrosion inhibition efficiency on carbon steel in formation water." *Egypt J Pet* (2017) 26: 41–51.
4. Hernández-Espejel, A, Domínguez-Crespo MA, Cabrera-Sierra R and Rodríguez-Meneses C, et al. "Investigations of corrosion films formed on API-X52 pipeline steel in acid sour media." *Corros Sci* (2010) 52: 2258–67.
5. El Bribri, A, Tabyaoui M, Tabyaoui B and El Attari H, et al. "The use of Euphorbia falcata extract as eco-friendly corrosion inhibitor of carbon steel in hydrochloric acid solution." *Mater Chem Phys* (2013) 141: 240–7.
6. Abdul Rahiman, AFS and Sethumanickam S. "Corrosion inhibition, adsorption and thermodynamic properties of poly (vinyl alcohol-cysteine) in molar HCl." *Arab J Chem* (2017) 10: S3358–66.
7. Umoren, SA and Solomon MM. "Synergistic corrosion inhibition effect of metal cations and mixtures of organic compounds: A Review." *J Environ Chem Eng* (2017) 5: 246–73.
8. Chokshi, KK. "A Study of Inhibitor - Scale Interaction in Carbon Dioxide Corrosion of Mild Steel." *Thesis Ohio University* (2004).
9. Huilong, W, Jiashen Z. and Jing L. "Inhibition of the corrosion of carbon steel in hydrochloric acid solution by bisquaternary ammonium salt." *Anti-Corros Methods Mater* (2002) Vol.49(2): p.127
10. Mosayebi, B, Kazemeini M, Badakhshan A and Safekordi A. "Modelling of the effect of operational parameters and concentration of some corrosion inhibitors on the corrosion of carbon steel." *Anti-Corrosion Methods Mater* (2002) 49: 426–32.
11. El Hamdani, N, Fdil R, Tourabi M and Jama C, et al. "Alkaloids extract of Retama monosperma (L.) Boiss. seeds used as novel eco-friendly inhibitor for carbon steel corrosion in 1 M HCl solution: Electrochemical and surface studies." *Appl Surf Sci* (2015) 357: 1294–305.
12. Shahabi, S, Norouzi P and Ganjali MR. "Electrochemical and theoretical study of the inhibition effect of two synthesized thiosemicarbazide derivatives on carbon steel corrosion in hydrochloric acid solution." *RSC Adv* (2015) 5: 20838–47.
13. Hemapriya, V, Prabakaran M, Parameswari K and Chitra S, et al. "Experimental and theoretical studies on inhibition of benzothiazines against corrosion of mild steel in acidic medium." *Anti-Corrosion Methods Mater* (2017) 64: ACMM-07-2015-1562.
14. Yahya, S, Othman NK, Daud AR and Jalar A, et al. "The influence of temperature on the inhibition of carbon steel corrosion in acidic lignin." *Anti-Corrosion Methods Mater* (2015) 62: 301–6.
15. Corro- E. "Measurements AP, Test- C, Environment HP, Inhibitors FC, Fluids S." *Standard Guide for Inhibitors in the Laboratory 1* (2018) 06: 1–16.
16. Ugur, D, Sonke J and Laycock N. "Corrosion and corrosion inhibition in wet gas pipelines." *Corros Mater* (2017) 42: 64–9.
17. Nyborg, R. "Controlling Internal Corrosion in Oil and Gas Pipelines." *Oil Gas Rev* (2005): 70–4.

18. Figure, Z, The O. "Surface preparation Preparation of test solutions Water and hydrocarbons Gas supply Corrosion rate measurements Electrochemical corrosion rate measurements." n.d.
19. Group S and Units O. "Appendix 2 Vendor information Pre-qualification tests." n.d.
20. Silveri, MA. "data sheet of Corrosion inhibitor." 2004.
21. "PRODUCT OVERVIEW CRONOX CRW9258 Corrosion Inhibitor General purpose corrosion inhibitor." 2014.
22. Abd El-Maksoud, SA and Fouda AS. "Some pyridine derivatives as corrosion inhibitors for carbon steel in acidic medium." *Mater Chem Phys* (2005) 93: 84–90.
23. Gadala, IM and Alfantazi A. "Electrochemical behavior of API-X100 pipeline steel in NS4, near-neutral and mildly alkaline pH simulated soil solutions." *Corros Sci* (2014) 82: 45–57.
24. Kabir, KB and Mahmud I. "Study of Erosion-Corrosion of Stainless Steel, Brass and Aluminum by Open Circuit Potential Measurements." *J Chem Eng* (2011) 25: 13–7.
25. Rehim, SSA, Hazzazi OA, Amin MA and Khaled KF. "On the corrosion inhibition of low carbon steel in concentrated sulphuric acid solutions. Part I: Chemical and electrochemical (AC and DC) studies." *Corros Sci* (2008) 50: 2258–71.
26. Abd El-raouf, M, El-Azabawy OE and El-Azabawy RE. "Investigation of adsorption and inhibitive effect of acid red GRE (183) dye on the corrosion of carbon steel in hydrochloric acid media." *Egypt J Pet* (2015) 24: 233–9.
27. Fattah-alhosseini, A and Noori M. "Corrosion inhibition of SAE 1018 carbon steel in H₂S and HCl solutions by lemon verbena leaves extract." *Meas J Int Meas Confed* (2016) 94: 787–93.
28. Ivušić, F, Lahodny-šarc O and Stojanović I. "Corrosion Inhibition of Carbon Steel in Saline Solutions By Gluconate, Zinc Sulphate and Clay Eluate." *Teh Vjesn* (2000) 3651: 107–14.
29. Desimone, MP, Gordillo G and Simison SN. "The effect of temperature and concentration on the corrosion inhibition mechanism of an amphiphilic amido-amine in CO₂ saturated solution." *Corros Sci* (2011) 53: 4033–43.
30. Tourir, R, Cenoui M, El Bakri M and Ebn Touhami M. "Sodium gluconate as corrosion and scale inhibitor of ordinary steel in simulated cooling water." *Corros Sci* (2008) 50: 1530–7.
31. Sun, W, Nešić S and Papavinasam S. "Kinetics of Iron Sulfide and Mixed Iron Sulfide/Carbonate Scale Precipitation in CO₂/H₂S Corrosion." *Corros NACE Expo* (2006): No.06644.
32. Lucio-Garcia, MA, Gonzalez-Rodriguez JG, Martinez-Villafañe A and Dominguez-Patiño G, et al. "A study of hydroxyethyl imidazoline as H₂S corrosion inhibitor using electrochemical noise and electrochemical impedance spectroscopy." *J Appl Electrochem* (2010) 40: 393–9.
33. Lucio-Garcia, MA, Gonzalez-Rodriguez JG, Casales M and Martinez L, et al. "Effect of heat treatment on H₂S corrosion of a micro-alloyed C-Mn steel." *Corros Sci* (2009) 51: 2380–6.
34. Hafiz, M, Afif R and Anaee M. "Republic of Iraq University of Technology A thesis Submitted To The Department of Materials Engineering, University of Technology in Partial Fulfillment of the Requirements for the Degree of Master of Science in Material Engineering By Rana S." *N Supervi* (2013).
35. Ousslim, A, Chetouani A, Hammouti B and Bekkouch K, et al. "Thermodynamics, quantum and electrochemical studies of corrosion of iron by piperazine compounds in sulphuric acid." *Int J Electrochem Sci* (2013) 8: 5980–6004.
36. Zulfareen, N, Kannan K, Venugopal T and Gnanavel S. "Synthesis, characterization and corrosion inhibition efficiency of N-(4-(Morpholinomethyl Carbamoyl Phenyl) Furan-2-Carboxamide for brass in HCl medium." *Arab J Chem* (2016) 9: 121–35.
37. Amini, M, M Aliofkhaezrai and AH Navidi Kashani ASR. "Mild Steel Corrosion Inhibition by Benzotriazole in 0.5M Sulfuric Acid Solution on Rough and Smooth Surfaces." *Int J Electrochem Sci* (2017) 12: 8708–32.
38. Alaneme, KK, Olusegun SJ and Adelowo OT. "Corrosion inhibition and adsorption mechanism studies of *Hunteria umbellata* seed husk extracts on mild steel immersed in acidic solutions." *Alexandria Eng J* (2016) 55: 673–81.
39. Khan, G, Basirun WJ, Kazi SN and Ahmed P, et al. "Electrochemical investigation on the corrosion inhibition of mild steel by Quinazoline Schiff base compounds in hydrochloric acid solution." *J Colloid Interface Sci* (2017) 502: 134–45.
40. Liu, QY, Mao LJ and Zhou SW. "Effects of chloride content on CO₂ corrosion of carbon steel in simulated oil and gas well environments." *Corros Sci* (2014) 84: 165–71.
41. Xiao, H, Ye W, Song X and Ma Y, et al. "Evolution of akaganeite in rust layers formed on steel submitted to wet/dry cyclic tests." *Materials (Basel)* (2017) 10: 1–14.
42. Sherif, ESM. "A comparative study on the electrochemical corrosion behavior of iron and X-65 steel in 4.0 wt % sodium chloride solution after different exposure intervals." *Molecules* (2014) 19: 9962–74.
43. Znini, M, Majidi L, Laghchimi A and Paolini J, et al. "Chemical composition and anticorrosive activity of Warionia saharea essential oil against the corrosion of mild steel in 0.5 M H₂SO₄." *Int J Electrochem Sci* (2011) 6: 5940–55.
44. Ma, H, Cheng X, Chen S and Wang C, et al. "An ac impedance study of the anodic dissolution of iron in sulfuric acid solutions containing hydrogen sulfide." *J Electroanal Chem* (1998) 451: 11–7.
45. Smith, SN and Brown B. "Corrosion at Higher H₂S Concentrations and Moderate Temperatures." *NACE Int* (2011): 1–18.
46. Roberge, P. "Corrosion Inhibitors." *Handb Corros Eng* (1995): 833–62.
47. Genescá, J, Mendoza J, Duran R and Garcia E. "Conventional Dc Electrochemical Techniques in Corrosion Testing." *XV Int Corros Congr* (2002).
48. Ma, H, Cheng X, Li G and Chen S, et al. "The influence of hydrogen sulfide on corrosion of iron under different conditions." *Corros Sci* (2000) 42: 1669–83. [https://doi.org/10.1016/S0010-938X\(00\)00003-2](https://doi.org/10.1016/S0010-938X(00)00003-2).
49. Bai, P, Zheng S and Chen C. "Electrochemical characteristics of the early corrosion stages of API X52 steel exposed to H₂S environments." *Mater Chem Phys* (2015) 149–150: 295–301.
50. Khaksar, L, Whelan G and Shirokoff J. "Electrochemical and Microstructural Analysis of FeS Films from Acidic Chemical Bath at Varying Temperatures, pH. Immersion Time (2016).
51. Vuković, M, Pesic B, Štrbac N and Mihajlović I, et al. "Linear Polarization Study of the Corrosion of Iron in the Presence of Thiobacillus ferrooxidans." *Bacteria* (2012) 7: 2487–503.
52. Chong, AL, Mardel JI, MacFarlane DR and Forsyth M, et al. "Synergistic Corrosion Inhibition of Mild Steel in Aqueous Chloride Solutions by an Imidazolium Carboxylate Salt." *ACS Sustain Chem Eng* (2016) 4: 1746–55.
53. Papavinasam, S. "Corrosion Inhibitors. In: *Uhlig's Corrosion Handbook. Second Edition* (2000).
54. Nady, H, El-Rabiei MM and Samy M. "Corrosion behavior and electrochemical properties of carbon steel, commercial pure titanium, copper and copper-aluminum-nickel alloy in 3.5% sodium chloride containing sulfide ions." *Egypt J Pet* (2017) 26: 79–94.
55. Jafari, H and Akbarzade K. "Effect of Concentration and Temperature on Carbon Steel Corrosion Inhibition." *J Bio- Tribo-Corrosion* (2017) 3: 1–9.
56. Amin, MA, Abd El Rehim SS and Abdel-Fatah HTM. "Electrochemical frequency modulation and inductively coupled plasma atomic emission spectroscopy methods for monitoring corrosion rates and inhibition of low alloy steel corrosion in HCl solutions and a test for validity of the Tafel extrapolation method." *Corros Sci* (2009) 51: 882–94.
57. León, LDL, Rodríguez MAV, Cruz VER and Calderón FA, et al. "Corrosion of carbon steel in presence of hydrocarbon." *Int J Electrochem Sci* (2011) 6: 3497–507.
58. Lebrini, M, Traisnel M, Lagrenée M and Mernari B, et al. "Inhibitive properties, adsorption and a theoretical study of 3,5-bis(n-pyridyl)-4-amino-1,2,4-triazoles as corrosion inhibitors for mild steel in perchloric acid." *Corros Sci* (2008) 50: 473–9.
59. Karthikaiselvi, R and Subhashini S. "Study of adsorption properties and inhibition of mild steel corrosion in hydrochloric acid media by water soluble composite poly (vinyl alcohol-o-methoxy aniline)." *J Assoc Arab Univ Basic Appl Sci* (2014) 16: 74–82.

How to cite this article: Noora Al Qahtani, Jiahui Qi, Aboubakr M. Abdullah, and Nicholas J. Laycock, et al. "Scales Formation Inhibition on Top of C-Steel in Sour Media; A Chemical and Electrochemical Study". *J Material Sci Eng* 10 (2021)